An accurate Local Average Contact method for nonmatching meshes.

Guillaume DROUET [1] [2] and Patrick HILD [2]

Abstract

The present paper deals with linear and quadratic finite element approximations of the two and three-dimensional unilateral contact problems between two elastic bodies with nonmatching meshes. We propose a simple noninterpenetration condition on the displacements which is local as the well known node-to-segment and node-to-face conditions and accurate like the mortar approach. This condition consists of averaging locally on a few elements the noninterpenetration. We prove optimal convergence rates in 2D and 3D using various linear and quadratic elements. The Taylor patch test and the Hertzian contact test illustrate the theoretical results and show the capabilities of the method.

Keywords. Unilateral contact, nonmatching meshes, a priori error estimates, Local Average Contact (LAC) condition, node-to-segment contact, node-to-face contact, mortar contact.

Abbreviated title. Local Average Contact (LAC)

AMS subject classifications. 35J86, 65N30.

1 Introduction and problem set-up

Finite element methods are currently used to approximate the unilateral contact problems, see, *e.g.*, [29, 37, 42, 57, 59]. Such problems show a nonlinear boundary condition, which roughly speaking requires that (a component of) the solution u is nonpositive on a part of the boundary of the domain Ω, see [50]. This nonlinearity leads to a weak formulation written as a variational inequality which admits a unique solution, (see [25]) and the regularity of the solution shows limitations whatever the regularity of the data is, see [45]. A consequence is that only finite element methods of order one and of order two are of interest which is the scope of this work.

This paper is focused on the contact configurations of two bodies whose respective meshes do not coincide on the contact interface, i.e., "nonmatching meshes". This situation often occurs in engineering computations since the different bodies are generally meshed in an independent way and the resulting discretizations do not fit together. In dynamic computations this situation also occurs at any time step and nonmatching meshes need to be handled if one wants to avoid remeshing with matching meshes at any time step. The contact problems with nonmatching meshes have been considered and studied from a theoretical point of view in the last twenty years. It is now known that the local node-to-segment contact conditions in 2D or the equivalent node-to-face conditions in 3D produce solutions with oscillations which degrade the accuracy and slow down the convergence of the computations. On the contrary the mortar domain decomposition method [10] handles in an optimal way the nonmatching meshes and its adaptation to contact problems gave promising theoretical and numerical results at the end of the 90's, see [4, 6, 7, 32, 33]. To summarize, this initial approach directly inspired from [10], considered a global

[1] *Institut des Sciences de la Mécanique et Applications Industrielles, UMR 9219 EDF-CNRS-CEA-ENSTA, Université Paris Saclay, 828 Boulevard des Maréchaux, 91762 Palaiseau Cedex France, guillaume.drouet@edf.fr*

[2] *Institut de Mathématiques de Toulouse, UMR 5219 (CNRS/Universités Toulouse 1,2,3/INSA Toulouse), Université Paul Sabatier (Toulouse 3), 118 route de Narbonne, 31062 Toulouse Cedex 9, France, phild@math.univ-toulouse.fr.*

L^2 projection of linear finite element functions from a mesh to another mesh on the contact area in two-dimensions. From a numerical point of view, this mortar concept has been adapted and extended to many contact configurations such as friction, quadratic finite elements, large deformations, three-dimensional problems... see, *e.g.* [13, 15, 19, 24, 28, 39, 43, 46, 47, 48, 53, 54, 56, 58] and the references therein.

Our aim in this study, is to propose the simplest contact condition which on the one hand gives optimal convergence results in the energy norm and on the other hand can be easily implemented in a industrial finite element code for various finite elements (3 and 6-node triangles, 4 and 8-node quadrangles in 2D and 4 and 10-node tetrahedra, 8, 20 and 27-node hexahedra in 3D). So we consider a discrete contact condition which requires, that the jump of the displacement denoted $[u_N^h]$ is nonpositive in average on some local patches (comprising one or several contact elements of one of the trace meshes) that form a partition of the contact zone and we call this approach Local Average Contact (LAC). The main benefit of this approach is that it naturally leads to a local method which makes the implementation in an industrial FE code easier, in particular ***Code_Aster*** [18] in which we are interested. The paper is organized as follows:

- Section 2 deals with the two-dimensional unilateral contact problem between two elastic bodies in the general case of nonmatching meshes. First, we introduce a new operator denoted π_1^h which locally preserves the average on the contact zone. We then perform the error analysis of the problem using the LAC condition on any patch. The results proved in this section are optimal without using any other assumption than the Sobolev regularity of the solution of the continuous problem.

- In section 3, we extend the previous results to the three-dimensional case without any loss on the convergence rates using only one mesh requirement hypothesis. This assumption can be easily fulfilled from a practical point of view.

- Section 4 is devoted to establish the links between our contact condition and an equivalent formulation with Lagrange multipliers: we introduce the corresponding mixed formulation of the problem using the LAC condition, and then discuss on the inf-sup condition which holds.

- In section 5, we show some numerical results of the method implemented in the industrial study and research finite element software of Electricité de France (EDF), ***Code_Aster***. The Taylor patch test and the Hertz contact are considered. These computations involve 3 and 6-node triangles, 4 and 8-node quadrangles in 2D and 4 and 10-node tetrahedra, 8, 20 and 27-node hexahedra in 3D.

Next, we specify some notations we shall use. Let ω be a Lebesgue-measurable subset of $\mathbb{R}^d$ with nonempty interior ; the generic point of ω is denoted x. The classical Lebesgue space $L^2(\omega)$ and the standard Sobolev space $H^m(\omega)$, $m \in \mathbb{N}$ (we adopt the convention $H^0(\omega) = L^2(\omega)$) are endowed with the norms:

$$\|\psi\|_{L^2(\omega)} = \left(\int_\omega |\psi(x)|^2 \, dx \right)^{1/2}, \quad \|\psi\|_{m,\omega} = \left(\sum_{0 \le |\alpha| \le m} \|\partial^\alpha \psi\|^2_{L^2(\omega)} \right)^{1/2},$$

where $\alpha = (\alpha_1, \ldots, \alpha_d)$ is a multi–index in $\mathbb{N}^d, |\alpha| = \alpha_1 + \cdots + \alpha_d$ and the symbol ∂^α represents a partial derivative. The fractional Sobolev space $H^\tau(\omega), \tau \in \mathbb{R}_+ \setminus \mathbb{N}$ with $\tau = m + \nu, m$ being

the integer part of τ and $\nu \in (0,1)$ is defined by the norm, see [3]:

$$\|\psi\|_{\tau,\omega} = \left(\|\psi\|^2_{m,\omega} + \sum_{|\alpha|=m} |\partial^\alpha \psi|^2_{\nu,\omega} \right)^{1/2},$$

where for $\nu \in (0,1)$ the seminorm is defined by:

$$|\psi|_{\nu,\omega} = \left(\int_\omega \int_\omega \frac{(\psi(x) - \psi(y))^2}{|x-y|^{d+2\nu}} \, dx \, dy \right)^{1/2}.$$

Let Ω^1 and Ω^2 in $\mathbb{R}^d$ $(d = 2, 3)$ stand for two polygonal or polyhedral domains representing the reference configurations of two linearly elastic bodies. The boundaries $\partial\Omega^\ell, \ell = 1, 2$ consist of three nonoverlapping open parts $\Gamma^\ell_{_N}$, $\Gamma^\ell_{_D}$ and Γ^ℓ_C with $\overline{\Gamma^\ell_{_N}} \cup \overline{\Gamma^\ell_{_D}} \cup \overline{\Gamma^\ell_C} = \partial\Omega^\ell$. We assume that the measures in $\mathbb{R}^{d-1}$of Γ^ℓ_C and $\Gamma^\ell_{_D}$ are positive. The bodies are submitted to a Neumann condition on $\Gamma^\ell_{_N}$ with a density of loads $F_\ell \in (L^2(\Gamma^\ell_{_N}))^d$, a Dirichlet condition on $\Gamma^\ell_{_D}$ (the bodies are assumed to be clamped on $\Gamma^\ell_{_D}$ to simplify) and to volume loads denoted $f_\ell \in (L^2(\Omega^\ell))^d$ in Ω^ℓ. Moreover we suppose to simplify that in the initial configuration the bodies have a common contact surface denoted Γ_C such that $\Gamma_C := \Gamma^1_C = \Gamma^2_C$ and that the final contact area after deformation is a subset of Γ_C. In the more general case where the final contact area is not expected to be a subset of the initial contact area, we would need to define a gap function g (generally on Γ^1_C or on Γ^2_C) representing the distance between both bodies. Finally, a frictionless unilateral contact condition between the bodies holds on Γ_C.

The problem consists in finding the displacement field $u = (u_1, u_2) : \overline{\Omega^1} \times \overline{\Omega^2} \to \mathbb{R}^d$ satisfying (1)–(6) with $\ell = 1, 2$:

$$-\text{ div } \sigma(u_\ell) = f_\ell \qquad \text{in } \Omega^\ell, \tag{1}$$

$$\sigma(u_\ell) = \mathcal{A}_\ell \varepsilon(u_\ell) \qquad \text{in } \Omega^\ell, \tag{2}$$

$$\sigma(u_\ell) n_\ell = F_\ell \qquad \text{on } \Gamma^\ell_{_N}, \tag{3}$$

$$u_\ell = 0 \qquad \text{on } \Gamma^\ell_{_D}, \tag{4}$$

where n_ℓ stands for the outward unit normal to Ω^ℓ on $\partial\Omega^\ell$, $\sigma(u_\ell)$ represents the stress tensor field, $\varepsilon(u_\ell) = (\nabla u_\ell + (\nabla u_\ell)^T)/2$ denotes the linearized strain tensor field, and $\mathcal{A}_\ell$ is the fourth order elastic coefficient tensor which satisfies the usual symmetry and ellipticity conditions and whose components are in $L^\infty(\Omega^\ell)$.

On Γ_C, we decompose the displacement and the stress vector fields in normal and tangential components as follows:

$$u_{\ell_{_N}} = u_\ell . n_\ell, \quad u_{\ell_{_T}} = u_\ell - u_{\ell_{_N}} n_\ell,$$

$$\sigma_{\ell_{_N}} = (\sigma(u_\ell) n_\ell) . n_\ell, \quad \sigma_{\ell_{_T}} = \sigma(u_\ell) n_\ell - \sigma_{\ell_{_N}} n_\ell,$$

and we denote by

$$[u_{_N}] = u_{1_{_N}} + u_{2_{_N}}$$

the jump of the normal displacement across the contact interface.

The unilateral contact condition on Γ_C is expressed by the following complementarity condition:

$$[u_{_N}] \leq 0, \quad \sigma_{_N} := \sigma_{1_{_N}} = \sigma_{2_{_N}} \leq 0, \quad [u_{_N}] \sigma_{_N} = 0, \tag{5}$$

where a vanishing gap between the two elastic solids has been chosen in the reference configuration. When the gap function g does not vanish the quantity $[u_{_N}]$ in (5) has to be changed with $[u_{_N}]-g$ where the jump is defined using a convenient parametrization.

The frictionless condition on Γ_C reads as: for $\ell = 1, 2$

$$\sigma_{\ell_{_T}} = 0. \tag{6}$$

Let us introduce the following Hilbert spaces:

$$V_\ell = \left\{ v_\ell \in (H^1(\Omega^\ell))^d : v = 0 \text{ on } \Gamma_{_D}^\ell \right\},$$

$$V = V_1 \times V_2.$$

The set of admissible displacements satisfying the noninterpenetration conditions on the contact zone is:

$$K = \{ v \in V : [v_{_N}] \leq 0 \quad \text{on } \Gamma_C \}.$$

Let be given the following forms for any $u = (u_1, u_2)$ and $v = (v_1, v_2)$ in V:

$$a(u,v) = \sum_{\ell=1}^{2} \int_{\Omega^\ell} \mathcal{A}_\ell \varepsilon(u_\ell) : \varepsilon(v_\ell)\, d\Omega^\ell, \quad l(v) = \sum_{\ell=1}^{2} \int_{\Omega^\ell} f_\ell . v_\ell \, d\Omega^\ell + \int_{\Gamma_{_N}^\ell} F_\ell . v_\ell \, d\Gamma^\ell.$$

From the previous assumptions it follows that $a(\cdot,\cdot)$ is a bilinear symmetric V-elliptic and continuous form on $V \times V$ and l is a linear continuous form on V. The weak formulation of Problem (1)–(6) is:

$$\begin{cases} \text{Find } u \in K \text{ satisfying:} \\ a(u, v-u) \geq l(v-u), \quad \forall\, v \in K. \end{cases} \tag{7}$$

Problem (7) admits a unique solution according to Stampacchia's Theorem.

Remark 1 *It is known that the unilateral contact condition generates singularities at contact-noncontact transition points: the work in [45] is restricted to* $\mathbb{R}^2$ *and considers the Laplace operator on a polygonal domain and allows us to conclude that the solution to the Signorini problem is* $H^{5/2-\varepsilon}$ *regular in the neighborhood of* Γ_C*. If* Γ_C *is not straight, e.g.,* Γ_C *is a union of straight line segments, then additional singularities appear (see section 2.3 in [3] for a study in the two-dimensional case). In the three-dimensional case the references [2, 1, 27] prove local* $C^{1,1/2}$ *regularity results.*

2 The Local Average Contact (LAC) in two dimensions (d=2)

Let $V_\ell^h \subset V_\ell$ be a family of finite dimensional vector spaces indexed by h_ℓ coming from a regular family T_ℓ^h of triangulations or quadrangulations of the domain Ω^ℓ, $\ell = 1, 2$ (see [11, 14, 23]). The notation h_ℓ represents the largest diameter among all (closed) elements $T \in T_\ell^h$. We choose standard continuous and piecewise affine or quadratic functions, *i.e.*:

$$V_\ell^h = \left\{ v_\ell^h \in (C(\overline{\Omega}^\ell))^2 : v_\ell^h{}_{|_T} \in P_k(T), \forall T \in T_\ell^h, v_\ell^h = 0 \text{ on } \Gamma_{_D} \right\},$$

where $k = 1$ or $k = 2$. We set

$$V^h = V_1^h \times V_2^h.$$

To simplify we next suppose that the candidate contact area Γ_C is a straight line segment when $d = 2$ or a polygon when $d = 3$. The extension of all the theoretical results in this paper to the case where Γ_C is a union of straight line segments when $d = 2$ or a union of polygons when $d = 3$ could be easily made with additional notations. The discrete set of admissible displacements satisfying the average noninterpenetration conditions on the contact zone is given by

$$K^h = \left\{ v^h \in V^h : \int_{I^m} [v_N^h] \, d\Gamma \leq 0 \quad \forall I^m \in I^M \right\}. \tag{8}$$

When $k = 1$ then I^M is a one-dimensional macro-mesh constituted by macro-segments I^m comprising (see Definition 1 hereafter) two adjacent segments of $T_1^h \cap \Gamma_C$ (*i.e.*, the one-dimensional mesh on Γ_C inherited by T_1^h). When $k = 2$ then I^M is simply the trace mesh on Γ_C inherited by T_1^h. The only requirement (when $k = 1$ or $k = 2$) is that any element of I^M admits an internal degree of freedom. Note that we choose the trace mesh of T_1^h but the symmetrical definition of I^M using T_2^h could be another choice. The discrete variational inequality issued from (7) is

$$\left\{ \begin{array}{l} \text{Find } u^h \in K^h \text{ satisfying:} \\ a(u^h, v^h - u^h) \geq l(v^h - u^h), \quad \forall \, v^h \in K^h. \end{array} \right. \tag{9}$$

According to Stampacchia's Theorem, problem (9) admits also a unique solution.

Remark 2 *The approximation using a local average contact condition on the macro-mesh I^M is said to be nonconforming since obviously $K^h \not\subset K$.*

Remark 3 *We first give an answer to the question: "why this new method ?". Our aim is to propose a local contact condition (as the node-to-segment or the node-to-face methods) which retains the stability and the accuracy of mortar approaches.*

Note that even in the simplest case (matching meshes and k=1) our method does not reduce to the two most common contact conditions:

$$[v_N^h] \ \leq 0 \ \textit{on} \ \Gamma_C, \tag{10}$$

and

$$\int_{T \cap \Gamma_C} [v_N^h] d\Gamma \leq 0 \ \textit{on any contact element} \ T \cap \Gamma_C. \tag{11}$$

In fact we are not able to propose a method which is local, which reduces to (10) or (11) in the case of matching meshes and which gives optimal convergence rates in the case of nonmatching meshes. Nevertheless our approach is close to the one in (11) in which we slightly enlarge the area where the average is considered (a patch I^m of contact elements instad of a single contact segment $T \cap \Gamma_C$).

We recall that we are interested in a simple local approach for computational purposes, see the introduction, so the powerful modified mortar methods such as the dual one (see [36, 40, 46, 58]) are not the best solution in our case. The same remark also holds for the stabilized mixed methods as in [35]. These methods are either non-local or too complex to be implemented in an simple and generic way in an industrial FE code at the moment.

2.1 The average preserving operator

We are going to define an operator denoted π_1^h. We begin with the linear case $k = 1$ and the quadratic case $k = 2$ will then be handled straightforwardly. We then show that the operator π_1^h preserves the average on any macro-segment I^m, it is $H^s(\Gamma_C)$-stable for any $s \in [0, 1]$ and it fulfills other convenient properties. This operator will allow us to obtain an optimal approximation error term in the forthcoming error analysis. Let W_1^h be the normal trace space of V_1^h on Γ_C. We denote by x_i, $i = 1, ..., n$ the nodes of the triangulation T_1^h located on $\overline{\Gamma}_C$ and by ϕ_i the corresponding basis function of W_1^h. The support of ϕ_i (in $\overline{\Gamma}_C$) is denoted Δ_i. We also suppose that the trace mesh $T_1^h \cap \Gamma_C$ is quasi-uniform (although there exists some less restrictive assumptions, see, *e.g.*, [17]). We denote respectively h_c, h_i and h_{I^m} the largest mesh length on Γ_C, the length of the segment Δ_i and the length of the segment I^m. We denote by C a positive generic constant which does neither depend on the mesh size nor on the function v.

Definition 1 *Suppose that* $\overline{\Gamma_C} \cap \overline{\Gamma_D^1} = \emptyset$.
1. Assume that $n = 2p + 1$. *Set* $I^M = \{[x_1, x_3], [x_3, x_5], \cdots, [x_{n-2}, x_n]\}$. *The operator*

$$\pi_1^h : L^1(\Gamma_C) \longrightarrow W_1^h$$

is as follows: for any $v \in L^1(\Gamma_C)$, $\pi_1^h v$ *is defined locally on every* $I^m = [x_i, x_{i+2}] \in I^M$ *by*

$$\pi_1^h v = \sum_{j=i}^{i+2} \alpha_j(v)\phi_j,$$

where

$$\left\{ \begin{array}{l} \alpha_j(v) = \dfrac{\displaystyle\int_{\Delta_j} v \ d\Gamma}{|\Delta_j|}, j = i, i+2, \\ \alpha_{i+1}(v) = \dfrac{\displaystyle\int_{I^m} v \ d\Gamma - \int_{I^m} \alpha_i(v)\phi_i \ d\Gamma - \int_{I^m} \alpha_{i+2}(v)\phi_{i+2} \ d\Gamma}{\displaystyle\int_{I^m} \phi_{i+1} \ d\Gamma}. \end{array} \right. \tag{12}$$

2. Assume that $n = 2p$. *Set* $I^M = \{[x_1, x_3], [x_3, x_5], \cdots, [x_{n-5}, x_{n-3}], [x_{n-3}, x_n]\}$. *The definition of* $\pi_1^h v$ *on any* I^m *is the same as in (12) except for* $I^m = [x_{n-3}, x_n]$ *where*

$$\pi_1^h v = \sum_{j=n-3}^{n} \alpha_j(v)\phi_j,$$

with

$$\left\{ \begin{array}{l} \alpha_j(v) = \dfrac{\displaystyle\int_{\Delta_j} v \ d\Gamma}{|\Delta_j|}, j = n-3, n-2, n, \\ \alpha_{n-1}(v) = \dfrac{\displaystyle\int_{I^m} v \ d\Gamma - \int_{I^m} \alpha_{n-3}(v)\phi_{n-3} \ d\Gamma - \int_{I^m} \alpha_{n-2}(v)\phi_{n-2} \ d\Gamma - \int_{I^m} \alpha_n(v)\phi_n \ d\Gamma}{\displaystyle\int_{I^m} \phi_{n-1} \ d\Gamma}. \end{array} \right.$$

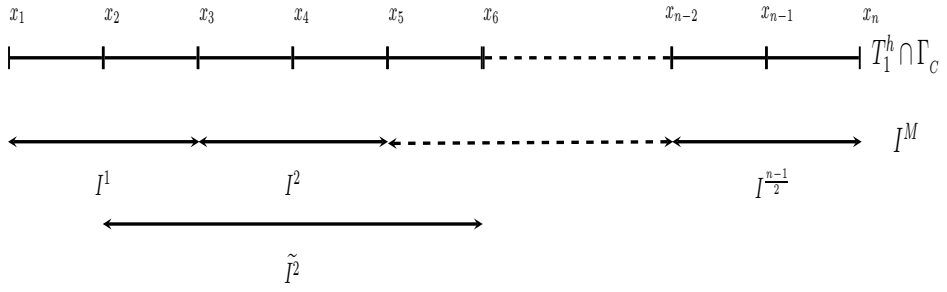

Figure 1: The trace mesh $T_1^h \cap \Gamma_C$ and the macro-mesh I^M.

Remark 4 *If $\overline{\Gamma_C} \cap \overline{\Gamma_D^1} \neq \emptyset$, the definition of I^M is done as in the previous definition depending on the even or odd number of contact segments on Γ_C. The only difference with the previous case in the definition of $\pi_1^h v$ comes from the Dirichlet condition on the boundary node x_1 and/or x_n. In that case we just need to define $\alpha_1(v) = 0$ and/or $\alpha_n(v) = 0$ so that π_1^h preserves the boundary conditions (i.e., $\pi_1^h v(x_1) = 0$ and/or $\pi_1^h v(x_n) = 0$).*

Proposition 1 *The operator π_1^h is linear and satisfies*

$$\int_{I^m} \pi_1^h v - v \; d\Gamma = 0, \; \forall v \in L^1(\Gamma_C), \; \forall I^m \in I^M.$$

Proof. The linearity of π_1^h is obvious, the average preserving property on I^m follows directly from the definition of π_1^h. ■

Proposition 2 *Let $\overline{\Gamma_C} \cap \overline{\Gamma_D} = \emptyset$. For any $s \in [0, 1]$, the operator π_1^h is $H^s(\Gamma_C)$-stable, i.e., there exists $C > 0$ such that for any $v \in H^s(\Gamma_C)$*

$$\|\pi_1^h v\|_{s,\Gamma_C} \leq C \|v\|_{s,\Gamma_C}.$$

Proof. First we show that for any $v \in L^2(\Gamma_C)$:

$$|\alpha_i(v)| \leq C h_c^{-\frac{1}{2}} \|v\|_{0,\tilde{I}^m}, \; \forall i = 1, \cdots, n, \tag{13}$$

where $\tilde{I}^m$ is the patch surrounding I^m: $\tilde{I}^m = \bigcup_{i:x_i \in I^m} \Delta_i$ (see Figure 1). Let $x_j \in I^m$, we have either

$$|\alpha_j(v)| \;=\; \left| \int_{\Delta_j} v \; d\Gamma \right| |\Delta_j|^{-1} \leq h_j^{-1} \int_{\Delta_j} |v| \; d\Gamma \leq h_j^{-\frac{1}{2}} \|v\|_{0,\Delta_j} \leq C h_c^{-\frac{1}{2}} \|v\|_{0,\tilde{I}^m} \tag{14}$$

or

$$\begin{aligned} |\alpha_j(v)| &= \left| \int_{I^m} v \; d\Gamma - \sum_{k \neq j : x_k \in I^m} \int_{I^m} \alpha_k(v) \phi_k \; d\Gamma \right| \left| \int_{I^m} \phi_j \; d\Gamma \right|^{-1} \\ &\leq C h_{I^m}^{-1} \left(h_{I^m}^{\frac{1}{2}} \|v\|_{0,I^m} + h_c^{\frac{1}{2}} \|v\|_{0,\tilde{I}^m} + h_c^{\frac{1}{2}} \|v\|_{0,\tilde{I}^m} \right) \\ &\leq C h_c^{-\frac{1}{2}} \|v\|_{0,\tilde{I}^m}, \end{aligned}$$

where we use (14) together with $|\phi_i| \leq 1$ on Γ_C and Cauchy-Schwarz inequality.

Next, we prove the local L^2-stability (on Γ_C) of π_1^h.

$$\begin{aligned} \|\pi_1^h v\|_{0,I^m} = \left\| \sum_{j:x_j \in I^m} \alpha_j(v)\phi_j \right\|_{0,I^m} \leq \sum_{j:x_j \in I^m} |\alpha_j(v)| \|\phi_j\|_{0,I^m} &\leq C h_{I^m}^{\frac{1}{2}} \sum_{j:x_j \in I^m} |\alpha_j(v)| \\ &\leq C\|v\|_{0,\tilde{I}^m}. \end{aligned} \tag{15}$$

So we deduce from (15) the $L^2(\Gamma_C)$-stability of π_1^h:

$$\|\pi_1^h v\|_{0,\Gamma_C}^2 = \sum_{I^m \in I^M} \|\pi_1^h v\|_{0,I^m}^2 \leq C \sum_{I^m \in I^M} \|v\|_{0,\tilde{I}^m}^2 \leq C\|v\|_{0,\Gamma_C}^2. \tag{16}$$

We now need to prove the $H^1(\Gamma_C)$-stability of π_1^h. We assume that $v \in H^1(\Gamma_C)$ and we show that

$$\|(\pi_1^h v)'\|_{0,\Gamma_C} \leq C\|v'\|_{0,\Gamma_C},$$

where the notation v' denotes the derivative of v. First we notice that

$$(\pi_1^h a)_{|_{I^m}} = a_{|_{I^m}}, \ \forall a \in P_0(\tilde{I}^m), \ \forall I^m \in I^M.$$

Using the definition of $\|(\pi_1^h v)'\|_{0,I^m}$, an inverse estimate and the local $L^2(I^m)$-stability (15) of π_1^h we get, for all $I^m \in I^M$ and all $a \in P_0(\tilde{I}^m)$:

$$\|(\pi_1^h v)'\|_{0,I^m} = \|(\pi_1^h (v-a))'\|_{0,I^m} \leq C h_{I^m}^{-1} \|\pi_1^h (v-a)\|_{0,I^m} \leq C h_{I^m}^{-1} \|v-a\|_{0,\tilde{I}^m}.$$

We set

$$a = |\tilde{I}^m|^{-1} \int_{\tilde{I}^m} v \ d\Gamma.$$

Using the standard inequality

$$\|v-a\|_{0,\tilde{I}^m} \leq C h_{\tilde{I}^m} \|v'\|_{0,\tilde{I}^m} \tag{17}$$

we deduce that

$$\|(\pi_1^h v)'\|_{0,I^m} \leq C\|v'\|_{0,\tilde{I}^m},$$

and by summation

$$\|(\pi_1^h v)'\|_{0,\Gamma_C} \leq C\|v'\|_{0,\Gamma_C}. \tag{18}$$

Thanks to (16) and (18), we obtain

$$\|\pi_1^h v\|_{1,\Gamma_C}^2 = \|\pi_1^h v\|_{0,\Gamma_C}^2 + \|(\pi_1^h v)'\|_{0,\Gamma_C}^2 \leq C(\|v\|_{0,\Gamma_C}^2 + \|v'\|_{0,\Gamma_C}^2) = C\|v\|_{1,\Gamma_C}^2. \tag{19}$$

Using the last bound together with (16) and an hilbertian interpolation argument (see [44, 55]) allows us to prove the $H^s(\Gamma_C)$-stability of π_1^h for all $s \in (0,1)$. ■

Remark 5 *If $\overline{\Gamma_C} \cap \overline{\Gamma_D^1} \neq \emptyset$, the previous results can be easily extended. Obviously the estimates (13), (15) and (16) still remain valid. Suppose first that $\overline{\Gamma_C} \cap \overline{\Gamma_N^1} = \emptyset$ (so $\alpha_1(v) = \alpha_n(v) = 0$) . In that case we need to prove that $\|(\pi_1^h v)'\|_{0,\Gamma_C} \leq C\|v'\|_{0,\Gamma_C}$ for $v \in H_0^1(\Gamma_C)$. This only requires to establish the local estimates $\|(\pi_1^h v)'\|_{0,I^m} \leq C\|v'\|_{0,\tilde{I}^m}$ for both extreme segments I^m containing*

x_1 and x_n (here π_1^h does not preserve the constant functions on the boundary segments). Since v vanishes on $\tilde{I}^m$, we write

$$\|(\pi_1^h v)'\|_{0,I^m} \leq C h_{I^m}^{-1} \|\pi_1^h v\|_{0,I^m} \leq C h_{I^m}^{-1} \|v\|_{0,\tilde{I}^m} \leq C \|v'\|_{0,\tilde{I}^m}.$$

This bound allows us to obtain estimate (18) *and then (19) for any $v \in H_0^1(\Gamma_C)$. The stability result in any interpolation space between $L^2(\Gamma_C)$ and $H_0^1(\Gamma_C)$ follows. The case where only one extremity of Γ_C is submitted to a Dirichlet condition is handled in a similar way.*

The extension to the quadratic case $k = 2$ is straightforward. The macro-mesh simply reduces to the trace mesh and π_1^h is defined on any quadratic segment $I^m = [x_i, x_{i+2}]$ as in Definition 1.1. in which the midpoint x_{i+1} allows to preserve the average. It is easy to check that Propositions 1, 2 and Remarks 4 and 5 still hold.

Remark 6 *The operator π_1^h does not preserve the continuous piecewise affine functions of W_1^h: if $v^h \in W_1^h$ then $\pi_1^h v^h \neq v^h$ in general, so π_1^h is not a projection operator. Moreover it is easy to check that π_1^h is not positivity preserving. Note that the operator π_1^h shows some similarities with the one in [12] (although π_1^h is average preserving whereas the operator in [12] preserves affine functions).*

2.2 Error analysis in two dimensions

The forthcoming theorem shows that the local average contact conditions in K^h give optimal convergence rates in the case of the unilateral contact of two elastic bodies with (and without) nonmatching meshes on the contact zone Γ_C. Denoting by $u = (u_1, u_2)$ with $u_\ell = u_{|_{\Omega^\ell}}$ we set $\|u\|^2_{s,\Omega^1,\Omega^2} = \|u_1\|^2_{s,\Omega^1} + \|u_2\|^2_{s,\Omega^2}$. We recall that h_1 and h_2 denote the largest mesh sizes of T_1^h and T_2^h.

Theorem 1 *Let u and u^h be the solutions to Problems (7) and (9) respectively. Assume that $u \in (H^\tau(\Omega^1))^2 \times (H^\tau(\Omega^2))^2$ with $3/2 < \tau \leq \min(k+1, 5/2)$, $k = 1, 2$. Then, there exists a constant $C > 0$ independent of h_1, h_2 and u such that*

$$\|u - u^h\|_{1,\Omega^1,\Omega^2} \leq C(h_1^{\tau-1} + h_2^{\tau-1}) \|u\|_{\tau,\Omega^1,\Omega^2}. \tag{20}$$

Remark 7 *Note that the same convergence rates could be proved for the standard mortar method applied to the two-dimensional unilateral contact between two elastic bodies when considering nonmatching meshes by using techniques of [21] and the standard tools from the mortar method. As already mentioned in the introduction our aim in this study is to propose a method where the noninterpenetration conditions are handled locally contrary to the standard mortar approach.*

Proof. The use of Falk's Lemma in the case $K^h \not\subset K$ gives (see, *e.g.*, [8]):

$$\begin{aligned} \alpha \|u - u^h\|^2_{1,\Omega^1,\Omega^2} \quad \leq \quad & \inf_{v^h \in K^h} \left(\|u - v^h\|^2_{1,\Omega^1,\Omega^2} + \int_{\Gamma_C} \sigma_{_N}[v^h_{_N} - u_{_N}] \, d\Gamma \right) \\ & + \inf_{v \in K} \int_{\Gamma_C} \sigma_{_N}[v_{_N} - u^h_{_N}] \, d\Gamma \end{aligned} \tag{21}$$

with $\alpha > 0$. First, we will prove that the approximation error, i.e., the first infimum in (21) is bounded in an optimal way. We choose $v^h \in V^h$ as follows

$$\begin{aligned} v_1^h &= I_1^h u_1 + R_1^h(\pi_1^h([u_{_N}] - I_1^h u_1.n_1 - I_2^h u_2.n_2)), \\ v_2^h &= I_2^h u_2, \end{aligned}$$

where I_ℓ^h is the Lagrange interpolation operator mapping onto V_ℓ^h, $\pi_1^h : L^1(\Gamma_C) \to W_1^h$ is the operator defined in the previous section and R_1^h is a discrete extension operator from W_1^h into V_1^h. Note that the discrete extension operators can be obtained by combining a standard continuous extension operator with a local regularization operator (see, e.g., [49, 9]). First, we show that v^h belongs to K^h. Let $I^m \in I^M$

$$\begin{aligned}
\int_{I^m} [v_{_N}^h]\ d\Gamma &= \int_{I^m} v_1^h.n_1 + v_2^h.n_2\ d\Gamma \\
&= \int_{I^m} I_1^h u_1.n_1 - \pi_1^h(I_1^h u_1.n_1)\ d\Gamma + \int_{I^m} I_2^h u_2.n_2 - \pi_1^h(I_2^h u_2.n_2)\ d\Gamma + \int_{I^m} \pi_1^h[u_{_N}]\ d\Gamma \\
&= \int_{I^m} \pi_1^h[u_{_N}]\ d\Gamma \\
&= \int_{I^m} [u_{_N}]\ d\Gamma \leq 0,
\end{aligned}$$

so $v^h \in K^h$. Then, thanks to the $H^{1/2}(\Gamma_C)$-stability of π_1^h (see Proposition 2), the trace theorem, and the Lagrange interpolation error estimates, the norm term of the approximation error is bounded in an optimal way:

$$\begin{aligned}
\|u - v^h\|_{1,\Omega^1,\Omega^2} &\leq \|u_1 - I_1^h u_1\|_{1,\Omega^1} + \|u_2 - I_2^h u_2\|_{1,\Omega^2} + \|R_1^h(\pi_1^h([u_{_N}] - I_1^h u_1.n_1 - I_2^h u_2.n_2))\|_{1,\Omega^1} \\
&\leq \|u_1 - I_1^h u_1\|_{1,\Omega^1} + \|u_2 - I_2^h u_2\|_{1,\Omega^2} + C\|\pi_1^h([u_{_N}] - I_1^h u_1.n_1 - I_2^h u_2.n_2)\|_{1/2,\Gamma_C} \\
&\leq \|u_1 - I_1^h u_1\|_{1,\Omega^1} + \|u_2 - I_2^h u_2\|_{1,\Omega^2} + C\|[u_{_N}] - I_1^h u_1.n_1 - I_2^h u_2.n_2\|_{1/2,\Gamma_C} \\
&\leq C(\|u_1 - I_1^h u_1\|_{1,\Omega^1} + \|u_2 - I_2^h u_2\|_{1,\Omega^2}) \\
&\leq C(h_1^{\tau-1} + h_2^{\tau-1})\|u\|_{\tau,\Omega^1,\Omega^2}, \quad 3/2 < \tau \leq k+1. \qquad (22)
\end{aligned}$$

In order to deal with the integral term of the approximation error, we consider the space X_1^h of the piecewise constant functions on the macro-mesh I^M:

$$X_1^h = \left\{ \chi^h \in L^2(\Gamma_C) : \chi^h{}_{|_{I^m}} \in P_0(I^m), \forall I^m \in I^M \right\},$$

and the classical $L^2(\Gamma_C)$-projection operator $\bar{\pi}_1^h : L^2(\Gamma_C) \to X_1^h$ defined for any $\varphi \in L^2(\Gamma_C)$ by

$$\int_{\Gamma_C} (\varphi - \bar{\pi}_1^h \varphi)\chi^h\ d\Gamma = 0, \quad \forall \chi^h \in X_1^h.$$

The operator $\bar{\pi}_1^h$ satisfies the following standard estimates for any $0 < r < 1$ and any $\varphi \in H^r(\Gamma_C)$ (see, e.g., [5]):

$$\|\varphi - \bar{\pi}_1^h \varphi\|_{0,\Gamma_C} + h_c^{-1/2}\|\varphi - \bar{\pi}_1^h \varphi\|_{1/2,*,\Gamma_C} \leq C h_c^r\, |\varphi|_{r,\Gamma_C}, \qquad (23)$$

where $\|.\|_{1/2,*,\Gamma_C}$ stands for the dual norm of $\|.\|_{1/2,\Gamma_C}$ and h_c is the maximal length of a trace segment on Γ_C. When $r = 0$ (resp. $r = 1$) the previous estimates remain true by changing $|\varphi|_{r,\cdot}$ with $\|\varphi\|_{0,\cdot}$ (resp. $\|\varphi'\|_{0,\cdot}$).

Since for all $I^m \in I^M$

$$\int_{I^m} ([u_{_N}] - I_1^h u_1.n_1 - I_2^h u_2.n_2) - \pi_1^h([u_{_N}] - I_1^h u_1.n_1 - I_2^h u_2.n_2)\ d\Gamma = 0,$$

we have:

$$\begin{aligned}
&\int_{\Gamma_C} \sigma_{_N} \left([v_{_N}^h] - [u_{_N}]\right)\, d\Gamma \\
= \;& -\int_{\Gamma_C} \sigma_{_N} \left([u_{_N}] - I_1^h u_1.n_1 - I_2^h u_2.n_2 - \pi_1^h([u_{_N}] - I_1^h u_1.n_1 - I_2^h u_2.n_2)\right)\, d\Gamma \\
= \;& -\int_{\Gamma_C} \left(\sigma_{_N} - \bar{\pi}_1^h \sigma_{_N}\right) \left([u_{_N}] - I_1^h u_1.n_1 - I_2^h u_2.n_2 - \pi_1^h([u_{_N}] - I_1^h u_1.n_1 - I_2^h u_2.n_2)\right)\, d\Gamma.
\end{aligned}$$

Finally, using Cauchy-Schwarz inequality, the $L^2(\Gamma_C)$-stability of π_1^h, the trace theorem, the Lagrange interpolation estimates and Young's inequality we get:

$$\begin{aligned}
&\int_{\Gamma_C} \sigma_{_N}([v_{_N}^h] - [u_{_N}])\, d\Gamma \\
\leq \;& \|\sigma_{_N} - \bar{\pi}_1^h \sigma_{_N}\|_{0,\Gamma_C} \|[u_{_N}] - I_1^h u_1.n_1 - I_2^h u_2.n_2 - \pi_1^h([u_{_N}] - I_1^h u_1.n_1 - I_2^h u_2.n_2)\|_{0,\Gamma_C} \\
\leq \;& C\|\sigma_{_N} - \bar{\pi}_1^h \sigma_{_N}\|_{0,\Gamma_C} \|[u_{_N}] - I_1^h u_1.n_1 - I_2^h u_2.n_2\|_{0,\Gamma_C} \\
\leq \;& C h_1^{\tau-3/2} |\sigma_{_N}|_{\tau-3/2,\Gamma_C} (h_1^{\tau-1/2} + h_2^{\tau-1/2}) \|u\|_{\tau,\Omega^1,\Omega^2} \\
\leq \;& C(h_1^{2(\tau-1)} + h_2^{2(\tau-1)}) \|u\|^2_{\tau,\Omega^1,\Omega^2}, \quad 3/2 < \tau \leq 5/2. \qquad (24)
\end{aligned}$$

Then, we need to optimally bound the consistency error, the second infimum in (21) in which we choose $v = 0$. The proof is long and technical and follows exactly the same lines as the consistency error analysis in [21], Theorems 1 and 2. Here we simply summarize this proof in a few lines. Since $\bar{\pi}_1^h \sigma_{_N}$ is a nonpositive piecewise constant function on Γ_C:

$$\begin{aligned}
-\int_{\Gamma_C} \sigma_{_N}[u_{_N}^h]\, d\Gamma \;&\leq\; -\int_{\Gamma_C} (\sigma_{_N} - \bar{\pi}_1^h \sigma_{_N})[u_{_N}^h]\, d\Gamma \\
&= \; -\int_{\Gamma_C} (\sigma_{_N} - \bar{\pi}_1^h \sigma_{_N})([u_{_N}^h] - [u_{_N}])\, d\Gamma - \int_{\Gamma_C} (\sigma_{_N} - \bar{\pi}_1^h \sigma_{_N})[u_{_N}]\, d\Gamma. \qquad (25)
\end{aligned}$$

The first term in (25) is bounded by using (23), the trace theorem and Young's inequality:

$$\begin{aligned}
-\int_{\Gamma_C} (\sigma_{_N} - \bar{\pi}_1^h \sigma_{_N})([u_{_N}^h] - [u_{_N}])\, d\Gamma \;&\leq\; \|\sigma_{_N} - \bar{\pi}_1^h \sigma_{_N}\|_{1/2,*,\Gamma_C} \|[u_{_N}^h] - [u_{_N}]\|_{1/2,\Gamma_C} \\
&\leq\; C h_1^{2(\tau-1)} \|u\|^2_{\tau,\Omega^1,\Omega^2} + \frac{\alpha}{2} \|u - u^h\|^2_{1,\Omega_1,\Omega_2}, 3/2 < \tau \leq 5/2. \qquad (26)
\end{aligned}$$

The second term in (25) is bounded on any macro-element $I^m \in I^M$. We denote by $Z_{_C}$ and $Z_{_{NC}}$ the contact and the noncontact sets in I^m respectively, i.e., $Z_{_C} = \{x \in I^m, [u_{_N}](x) = 0\}$, and $Z_{_{NC}} = \{x \in I^m, [u_{_N}](x) < 0\}$, and by $|Z_{_C}|$, $|Z_{_{NC}}|$ their measures in $\mathbb{R}$ (so $|Z_{_C}| + |Z_{_{NC}}| = h_{I^m}$). When $|Z_{_C}| > 0$ and $|Z_{_{NC}}| > 0$ (otherwise the integral term vanishes) we obtain (see [21]):

$$-\int_{I^m} (\sigma_{_N} - \bar{\pi}_1^h \sigma_{_N})[u_{_N}]\, d\Gamma \;\leq\; C \frac{h_{I^m}^{2\tau-3/2} \left(|\sigma_{_N}|^2_{\tau-3/2,I^m} + |[u_{_N}]'|^2_{\tau-3/2,I^m}\right)}{\max(|Z_{_C}|^{1/2}, |Z_{_{NC}}|^{1/2})}.$$

By noting that either $|Z_{_{NC}}|$ or $|Z_{_C}|$ is greater than $h_{I^m}/2$, summing over all the macro-elements I^m, and then using the trace theorem, we come to the conclusion that:

$$-\int_{\Gamma_C} (\sigma_{_N} - \bar{\pi}_1^h \sigma_{_N})[u_{_N}]\, d\Gamma \;\leq\; C h_1^{2(\tau-1)} \|u\|^2_{\tau,\Omega^1,\Omega^2}, \quad 3/2 < \tau \leq 5/2. \qquad (27)$$

Combining in (21) the approximation error estimates (22), (24) with the consistency error estimates (26), (27) allows us to obtain the optimal estimate (20). ■

3 The LAC in three dimensions (d=3)

In this section we extend the LAC approach to the three-dimensional case. The polyhedral domains Ω^1 and Ω^2 have a common candidate contact zone Γ_C which is is a polygon. We denote by $\mathcal{T}_\ell^h$ the regular tetrahedra or hexaheda family discretizing the domain Ω^ℓ and by h_ℓ the largest mesh size. In the following we will consider four nodes linear tetrahedra (TETRA 4), ten nodes quadratic tetrahedra (TETRA 10), eight nodes linear hexahedra (HEXA 8), twenty and twenty-seven nodes quadratic hexahedra (HEXA 20 and HEXA 27).

To deal with the error analysis we have to extend the definition of the operator π_1^h (see Definition 1) to the two-dimensional case. We also need that the main properties of π_1^h (linearity, average preserving, $H^s(\Gamma_C)$-stability) remain true in this case. We have to introduce the "internal degree of freedom hypothesis" which is needed to construct π_1^h and to carry out the convergence analysis.

Hypothesis 1 *(internal d.o.f.) There exists a macro-mesh T^M of Γ_C whose elements are unions of elements of $\mathcal{T}_\ell^h \cap \Gamma_C$ such that for every macro-element $T^m \in T^M$, there exists (at least) a degree of freedom x_i of V_ℓ^h such that* $\mathrm{supp}(\phi_i) \subset T^m$*, where ϕ_i is the basis function associated to x_i. Moreover there exists a constant C such that the largest mesh size of the macro-mesh is lower than Ch_ℓ (this last requirement is made to avoid a too coarse macro-mesh).*

From a theoretical point of view one could try to show that this hypothesis can be generally fulfilled by gathering some elements on Γ_C but such a strategy would not be interesting from a practical numerical point of view. We choose another strategy which consists of a local refinement of the contact mesh $\mathcal{T}_\ell^h \cap \Gamma_C$ whose aim is that the mesh $\mathcal{T}_\ell^h \cap \Gamma_C$ before refinement becomes the macro-mesh. For HEXA 27 elements, no refinement is needed and the trace mesh can be chosen as macro-mesh since there is already an internal degree of freedom. For the other elements the refinement strategy consists of adding (at least) an internal d.o.f. by refining the contact elements as suggested in Figure 2.

Remark 8 *1. The refinement strategy is local and only concerns the elements which have a face on the contact area (see Figure 3 where a tetrahedra mesh is refined).*

2. One can either choose to refine the mesh of one or of the other body.

3. The refinement does not affect the regularity and the quasi-uniformness properties of the meshes.

3.1 The average preserving operator

We next suppose that T^M is a macro-mesh of Γ_C satisfying Hypothesis 1 and built from the mesh of $\mathcal{T}_1^h \cap \Gamma_C$. Let W_ℓ^h be the normal trace space of $V_\ell^h = \{v_\ell^h \in (C(\overline{\Omega}^\ell))^3 : v_\ell^h{}_{|_\mathcal{T}} \in P_k(\mathcal{T}), \forall \mathcal{T} \in \mathcal{T}_\ell^h, v_\ell^h = 0 \text{ on } \Gamma_D\}$ on $\Gamma_C \subset \mathbb{R}^2$ with $k = 1, 2$. Let ϕ_i be the basis functions associated to the degrees of freedom of W_1^h. We denote x_i, $i = 1, .., n$ the corresponding nodes of $\mathcal{T}_1^h \cap \Gamma_C$ and $\Delta_i = \mathrm{supp}(\phi_i)$.

Definition 2 *Assume that Hypothesis 1 holds. The operator*

$$\pi_1^h : L^1(\Gamma_C) \longrightarrow W_1^h$$

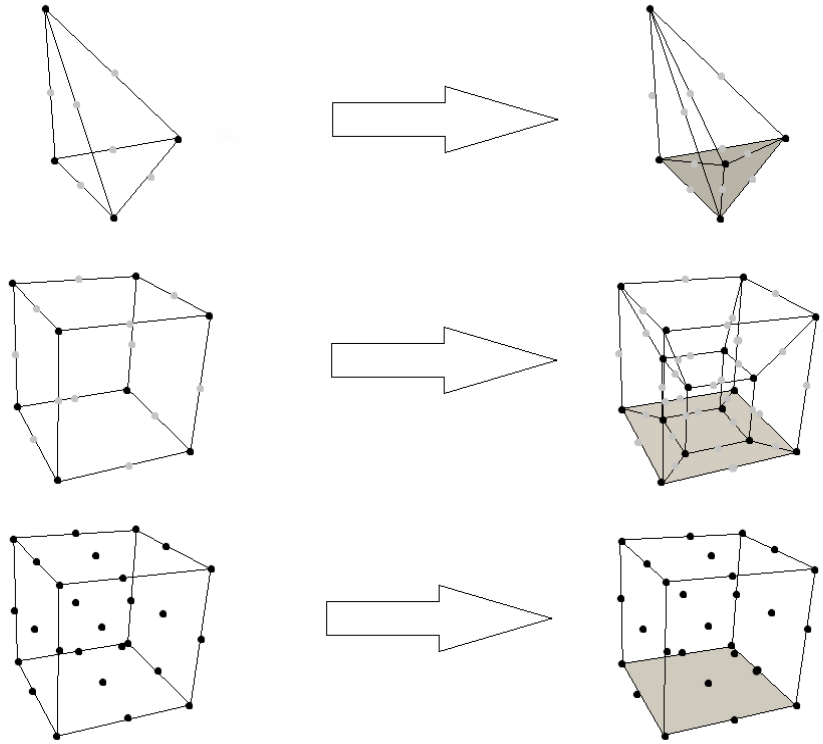

Figure 2: Upper picture: refinement strategy for linear (TETRA 4) and quadratic (TETRA 10) tetrahedra. Middle picture: refinement strategy for linear (HEXA 8) and quadratic (HEXA 20) hexahedra. Lower picture: for quadratic HEXA 27 hexahedra, no refinement is needed.

is as follows for any $v \in L^1(\Gamma_C)$. *If* x_i *is a node in* $\overline{\Gamma_C} \cap \overline{\Gamma_D^1}$, *then* $\pi_1^h v(x_i) = 0$. *Then* $\pi_1^h v$ *is defined locally on every macro-element* $T^m \in T^M$ *having as nodes* $x_i, i = 1, ..., m$ *(*$x_i \notin \overline{\Gamma_C} \cap \overline{\Gamma_D^1}$*) and as internal d.o.f.* x_{m+1} *by*

$$\pi_1^h v = \sum_{j=1}^{m+1} \alpha_j(v)\phi_j,$$

where

$$\begin{cases} \alpha_j(v) = \dfrac{\displaystyle\int_{\Delta_j} v \; d\Gamma}{|\Delta_j|}, j = 1, ..., m \\ \alpha_{m+1}(v) = \dfrac{\displaystyle\int_{T^m} v \; d\Gamma - \sum_{j=1}^{m} \int_{T^m} \alpha_j(v)\phi_j \; d\Gamma}{\displaystyle\int_{T^m} \phi_{m+1} \; d\Gamma}. \end{cases}$$

Remark 9 *1. If* T^M *contains more than one internal d.o.f. then we fix one of them which is denoted* x_{m+1} *and the other internal d.o.f. are handled as standard nodes.*

2. If we adopt the procedure depicted in Figure 2 when choosing TETRA 4, TETRA 10, HEXA 8, HEXA 20, HEXA 27 elements, we have respectively $m = 3, m = 9, m = 7, m = 19, m = 8$.

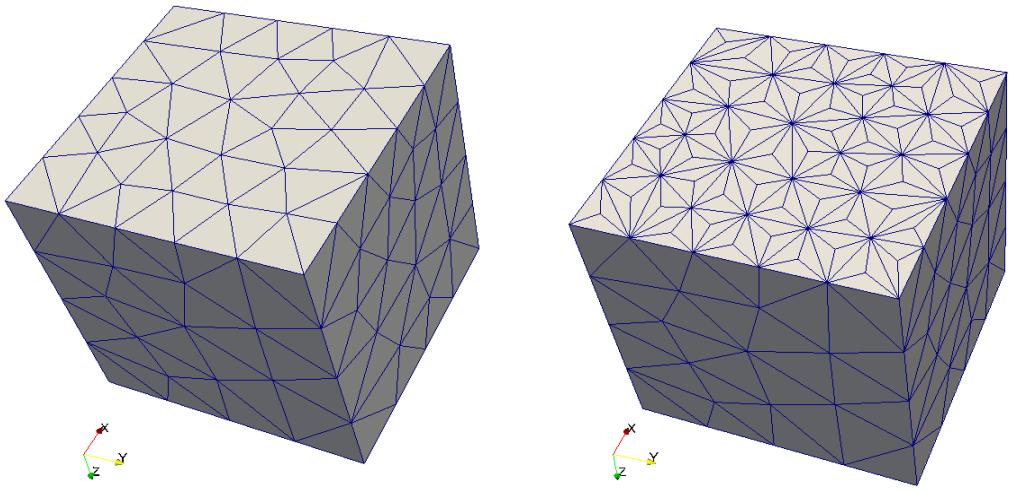

Figure 3: An example of a refinement on the $\vec{O}x\vec{O}y$ face of a cube which stands for Γ_C: the original mesh on the left side and the refined one on the right side.

Proposition 3 *1. The operator π_1^h is linear and satisfies*

$$\int_{T^m} \pi_1^h v - v \; d\Gamma = 0, \;\; \forall v \in L^1(\Gamma_C), \;\; \forall T^m \in T^M.$$

2. For any $s \in [0,1]$, the operator π_1^h is $H^s(\Gamma_C)$-stable, i.e., there exists $C > 0$ such that for any $v \in H^s(\Gamma_C)$

$$\|\pi_1^h v\|_{s,\Gamma_C} \leq C \|v\|_{s,\Gamma_C}.$$

Proof. The linearity of π_1^h is obvious. The average preserving property on T^m follows directly from the definition of π_1^h. When $\overline{\Gamma_C} \cap \overline{\Gamma_D^1} = \emptyset$ then the proof of the stability is obtained from a similar calculation as in the one-dimensional case. It is easy to check that for any j, we have

$$|\alpha_j(v)| \leq C|\Delta_j|^{-1/2} \|v\|_{0,\tilde{T}^m} \leq C h_c^{-1} \|v\|_{0,\tilde{T}^m} \tag{28}$$

where $\tilde{T}^m = \bigcup_{i:x_i \in T^m} \Delta_i$. Therefore the local L^2-stability: $\|\pi_1^h v\|_{0,T^m} \leq C\|v\|_{0,\tilde{T}^m}$ and hence the global L^2-stability $\|\pi_1^h v\|_{0,\Gamma_C} \leq C\|v\|_{0,\Gamma_C}$ follow. As in the one-dimensional case, the local L^2-stability of the gradient:

$$\|\nabla \pi_1^h v\|_{0,T^m} \leq C \|\nabla v\|_{0,\tilde{T}^m} \tag{29}$$

is a direct consequence of the property $\nabla \pi_1^h a = 0$ on T^m for all $a \in P_0(\tilde{T}^m)$ and of the error estimate (17) in two dimensions (see [5]).

When $\overline{\Gamma_C} \cap \overline{\Gamma_D^1} \neq \emptyset$, the estimate (28) remains true for any j. It suffices then to prove the local stability (29) still holds when T^m has at least a node in $\overline{\Gamma_D^1}$ (in that case the constant functions are not preserved on T^m). So

$$\|\nabla \pi_1^h v\|_{0,T^m} \leq C h_c^{-1} \|\pi_1^h v\|_{0,T^m} \leq C h_c^{-1} \|v\|_{0,\tilde{T}^m} \leq C \|\nabla v\|_{0,\tilde{T}^m}$$

where the last bound follows from Poincaré inequality and since v vanishes on a set of positive measure in $\partial\tilde{T}^m$. Denoting by $H^1_{0,\Gamma_D^1}(\Gamma_C)$ the functions of $H^1(\Gamma_C)$ vanishing on $\overline{\Gamma_C} \cap \overline{\Gamma_D^1}$, we deduce that π_1^h is stable in any interpolation space between $L^2(\Gamma_C)$ and $H^1_{0,\Gamma_D^1}(\Gamma_C)$. ■

3.2 Error analysis in three dimensions

The forthcoming result shows that the use of the discrete cone K^h of admissible displacements in the three-dimensional case (see definition hereafter) leads to optimal convergence in the energy norm. As previously, we set $\|u\|^2_{s,\Omega^1,\Omega^2} = \|u_1\|^2_{s,\Omega^1} + \|u_2\|^2_{s,\Omega^2}$ where $u = (u_1, u_2)$ and $u_\ell = u_{|_{\Omega^\ell}}$. We recall that $V^h = V_1^h \times V_2^h$ and we define K^h as

$$K^h = \left\{ v^h \in V^h : \int_{T^m} [v_N^h]\ d\Gamma \leq 0 \ \ \forall T^m \in T^M \right\}.$$

Let u^h be the unique solution of the three-dimensional discrete problem

$$\text{(30)} \qquad \begin{cases} \text{Find } u^h \in K^h \text{ satisfying:} \\ a(u^h, v^h - u^h) \geq l(v^h - u^h), \ \ \forall\ v^h \in K^h. \end{cases}$$

Theorem 2 *Let u and u^h be the solutions to Problems (7) and (30) respectively. Assume that Hypothesis 1 is verified and that $u \in (H^\tau(\Omega^1))^3 \times (H^\tau(\Omega^2))^3$ with $3/2 < \tau \leq \min(k+1, 5/2)$, $k = 1, 2$. Then, there exists a constant $C > 0$ independent of h_1, h_2 and u such that*

$$\|u - u^h\|_{1,\Omega^1,\Omega^2} \leq C(h_1^{\tau-1} + h_2^{\tau-1})\|u\|_{\tau,\Omega^1,\Omega^2}.$$

Remark 10 *For the "standard mortar" approach, we would need to take care of the extreme nodes of Γ_C in order to get the optimal convergence rate when considering nonmatching meshes. In fact the new result coming from [21] cannot be extended straightforwardly to the 3D "standard mortar" framework (contrary to the 2D case). Note that the method in the present paper does not have such limitations at the extreme nodes in the 3D case.*

Proof. From Falk's Lemma, we get the abstract error estimate (21). Due to the properties of π_h^1, we can bound the approximation error term in an optimal way as in the previous section by choosing $v^h \in V^h$ such that

$$\begin{aligned} v_1^h &= I_1^h u_1 + R_1^h(\pi_1^h([u_N] - I_1^h u_1.n_1 - I_2^h u_2.n_2)), \\ v_2^h &= I_2^h u_2. \end{aligned}$$

As in the two-dimensional case it is easy to check that $v^h \in K^h$ and to obtain the bound for the approximation error when $3/2 < \tau \leq \min(k+1, 5/2)$:

$$\inf_{v^h \in K^h} \left(\|u - v^h\|^2_{1,\Omega^1,\Omega^2} + \int_{\Gamma_C} \sigma_N [v_N^h - u_N]\ d\Gamma \right) \leq C(h_1^{2(\tau-1)} + h_2^{2(\tau-1)})\|u\|^2_{\tau,\Omega^1,\Omega^2}.$$

The consistency error is handled as in the two-dimensional case by using the techniques of [21]. We obtain for $3/2 < \tau \leq 5/2$:

$$\inf_{v \in K} \int_{\Gamma_C} \sigma_N [v_N - u_N^h]\ d\Gamma \leq C h_1^{2(\tau-1)} \|u\|^2_{\tau,\Omega^1,\Omega^2} + \frac{\alpha}{2}\|u - u^h\|^2_{1,\Omega_1,\Omega_2}.$$

Both previous bounds and (21) prove the theorem. ■

4 The mixed formulation of the LAC method

First, we introduce the equivalent mixed formulation of the variational inequality problem using the LAC condition. Then we will discuss on the link between the macro-mesh of the contact zone (in particular Hypothesis 1) and the inf-sup condition.

4.1 The equivalent mixed formulation of the unilateral contact problem using the local average contact condition

Here we are going to show the link between the variational inequality methods ((9) when $d = 2$ and (30) when $d = 3$) using the local average noninterpenetration condition and the mixed formulation of the unilateral contact problem. We rather adopt the notations of the 3D case, in particular T^m, T^M but of course the analysis also applies to 2D when noting I^m, I^M for the macro-mesh.

Definition 3 *We recall that* $V^h = V_1^h \times V_2^h$ *where for* $d = 2, 3$ *and* $k = 1, 2$*:*

$$V_\ell^h = \left\{ v_\ell^h \in (C(\overline{\Omega}^\ell))^d : v_\ell^h{}_{|_\mathcal{T}} \in P_k(\mathcal{T}), \forall \mathcal{T} \in \mathcal{T}_\ell^h, v_\ell^h = 0 \text{ on } \Gamma_{_D} \right\}.$$

We choose piecewise constant nonpositive Lagrange multipliers on the macro-mesh T^M *on* Γ_C*, i.e., in the convex cone* M^h*:*

$$M^h = \{\mu^h \in X_1^h : \mu^h \leq 0 \text{ on } \Gamma_C\} \text{ where } X_1^h = \{\mu^h \in L^2(\Gamma_C) : \mu^h{}_{|_{T^m}} \in P_0(T^m), \forall T^m \in T^M\}.$$

We also introduce the bilinear form b *on* $X_1^h \times V^h$ *defined by*

$$b(\mu^h, v^h) = \int_{\Gamma_C} \mu^h [v_{_N}^h] \, d\Gamma.$$

Proposition 4 *Assume that Hypothesis 1 holds. The problem (30) (or (9) when* $d = 2$*) and the problem: find* $u^h \in V^h$ *and* $\lambda^h \in M^h$ *such that*

$$\begin{cases} a(u^h, v^h) - b(\lambda^h, v^h) = l(v^h), \ \forall v^h \in V^h, \\ b(\mu^h - \lambda^h, u^h) \geq 0, \ \forall \mu^h \in M^h, \end{cases} \tag{31}$$

are well-posed and equivalent, i.e., the solution u^h *of (30) (or (9) when* $d = 2$*) coincides with the first component of the solution of (31).*

Lemma 1 *Assume that Hypothesis 1 holds. Let* μ^h *belong to* X_1^h*. We have the following implication*

$$\int_{\Gamma_C} \mu^h [v_{_N}^h] \, d\Gamma = 0, \ \forall v^h \in V^h \Rightarrow \mu^h = 0.$$

Proof of the lemma. Let $\mu^h \in X_1^h$. It is sufficient to prove that for all $T^m \in T^M$

$$\mu^h{}_{|_{T^m}} = 0. \tag{32}$$

Let T^m belong to T^M. From Hypothesis 1, there exists ϕ_i such that $\text{supp}(\phi_i) \subset T^m$. Then, we set v^h so that $[v_{_N}^h] = \phi_i$. Since μ^h belongs to X_1^h, we have

$$0 = \int_{\Gamma_C} \mu^h [v_{_N}^h] \, d\Gamma = \int_{T^m} \mu^h \phi_i \, d\Gamma = \mu^h \int_{T^m} \phi_i \, d\Gamma.$$

So we obtain (32) ■

Proof of the proposition 4. First, we suppose that problem (31) is well-posed and we prove the equivalence between (30) (or (9) when $d = 2$) and (31). Let $(u^h, \lambda^h) \in V^h \times M^h$ be the solution of (31). We have,

$$b(\mu^h - \lambda^h, u^h) \geq 0, \ \forall \mu^h \in M^h.$$

Taking $\mu^h = 0$ and $\mu^h = 2\lambda^h$ leads to:

$$b(\lambda^h, u^h) = 0 \tag{33}$$

$$b(\mu^h, u^h) \geq 0, \ \forall \mu^h \in M^h. \tag{34}$$

Choosing in (34) $\mu^h = -1$ on T^m and $\mu^h = 0$ elsewhere allows us to conclude that $u^h \in K^h$. From (31) and (33), we get

$$a(u^h, u^h) = l(u^h), \tag{35}$$

and for any $v^h \in K^h$, we obtain

$$a(u^h, v^h) - l(v^h) = b(\lambda^h, v^h) \geq 0. \tag{36}$$

Putting together $u^h \in K^h$, (35) and (36) implies that u^h is a solution of Problem (30). Since the problems (30) and (31) are well-posed, they are equivalent.

Then, we show that Problem (31) is well-posed. The existence of the solution $(u^h, \lambda^h) \in V^h \times M^h$ of (31) and the uniqueness of u^h come from standard results (see, *e.g.*, [29]). It remains to prove the uniqueness of the multiplier λ^h with the help of Lemma 1. Let $(u^h, \lambda_1^h) \in V^h \times M^h$ and $(u^h, \lambda_2^h) \in V^h \times M^h$ be two solutions of (31). Therefore

$$a(u^h, v^h) - b(\lambda_1^h, v^h) = l(v^h), \ \forall v^h \in V^h, \tag{37}$$

$$a(u^h, v^h) - b(\lambda_2^h, v^h) = l(v^h), \ \forall v^h \in V^h. \tag{38}$$

By subtracting (38) from (37), we get

$$\int_{\Gamma_C} (\lambda_1^h - \lambda_2^h)[v_N^h] \, d\Gamma = 0, \forall v^h \in V^h.$$

Since $\lambda_1^h - \lambda_2^h$ belongs to X_1^h, the use of Lemma 1 gives us $\lambda_1^h = \lambda_2^h$. So, we obtain the uniqueness of λ^h and the well-posedness of (31). ■

4.2 The inf-sup condition

Now we see that Hypothesis 1 we use on the contact mesh ensures that the corresponding mixed method using piecewise constant Lagrange multipliers on the macro-mesh T^M (or I^M in 2D) verifies the inf-sup condition.

The inf-sup condition involved in our formulation is as follows: there is a constant β^h such that

$$\inf_{\mu^h \in X_1^h} \sup_{v^h \in V^h} \frac{b(\mu^h, v^h)}{\|\mu^h\|_{W'} \, \|v^h\|_{1,\Omega^1,\Omega^2}} \geq \beta^h > 0,$$

where W is the normal trace space on Γ_C issued from V_1 and W' denotes its dual. It is easy to check that Lemma 1 implies the existence of such a constant β^h. Moreover it is well known that the inf-sup constant β^h also arises in the error analysis of the mixed formulation (31). In order to get

the best convergence rate we need to prove that β^h is independent of the mesh size $h = (h_1, h_2)$. Next, we show the link between Hypothesis 1, the operator π_1^h and the mesh-independent inf-sup condition: there is a constant β such that:

$$\inf_{\mu^h \in X_1^h} \sup_{v^h \in V^h} \frac{b(\mu^h, v^h)}{\|\mu^h\|_{W'} \, \|v^h\|_{1,\Omega^1,\Omega^2}} \geq \beta > 0, \tag{39}$$

that is the aim of the following proposition.

Proposition 5 *There exists a positive constant β which does not depend on the mesh size such that: for all $\mu^h \in X_1^h$, there exists $v^h \in V^h$, $v^h \neq 0$ such that*

$$b(\mu^h, v^h) \geq \beta \|\mu^h\|_{W'} \|v^h\|_{1,\Omega^1,\Omega^2}. \tag{40}$$

Proof. Note first that (40) and (39) are equivalent. Let μ^h belong to X_1^h. Since $X_1^h \subset W'$, we can use the continuous inf-sup condition (see, *e.g.*, [29]): there is a constant $\tilde{\beta}$ such that

$$\inf_{\mu \in W'} \sup_{v \in V} \frac{b(\mu, v)}{\|\mu\|_{W'} \, \|v\|_{1,\Omega^1,\Omega^2}} \geq \tilde{\beta} > 0. \tag{41}$$

So, for all $\mu^h \in X_1^h$ there exists $v \in V$ such that:

$$b(\mu^h, v) \geq \tilde{\beta} \|\mu^h\|_{W'} \|v\|_{1,\Omega^1,\Omega^2}.$$

To prove (40) it is sufficient to show that there exists $v^h \in V^h$ satisfying the two following conditions:

$$b(\mu^h, v^h) = b(\mu^h, v), \tag{42}$$

$$\|v^h\|_{1,\Omega^1,\Omega^2} \leq C \|v\|_{1,\Omega^1,\Omega^2}. \tag{43}$$

In fact if (42) and (43) hold, we get (40) with $\beta = \tilde{\beta}/C$, *i.e.*,

$$b(\mu^h, v^h) = b(\mu^h, v) \geq \tilde{\beta} \|\mu^h\|_{W'} \|v\|_{1,\Omega^1,\Omega^2} \geq \frac{\tilde{\beta}}{C} \|\mu^h\|_{W'} \|v^h\|_{1,\Omega^1,\Omega^2}.$$

In order to satisfy the condition (42), we set $v^h = (v_1^h, v_2^h)$ such that

$$v_1^h = R_1^h \pi_1^h [v_N], \quad v_2^h = 0,$$

where R_1^h ia a discrete extension operator. Since π_1^h preserves the average on every macro-element T^m, v^h satisfies:

$$\int_{T^m} [v_N^h] \, d\Gamma = \int_{T^m} \pi_1^h [v_N] \, d\Gamma = \int_{T^m} [v_N] \, d\Gamma, \ \forall T^m \in T^M.$$

By summing over the T^m and since μ^h is constant on any T^m, we get (42):

$$b(\mu^h, v^h) = \int_{\Gamma_C} \mu^h [v_N^h] \, d\Gamma = \int_{\Gamma_C} \mu^h [v_N] \, d\Gamma = b(\mu^h, v).$$

To finish the proof, it remains to show that v^h verifies (43). Thanks to the $H^{\frac{1}{2}}(\Gamma_C)$-stability of π_1^h and the trace theorem, we have

$$\|v^h\|_{1,\Omega^1,\Omega^2} = \|R_1^h \pi_1^h [v_N]\|_{1,\Omega^1} \leq C \|\pi_1^h [v_N]\|_{1/2,\Gamma_C} \leq C \|[v_N]\|_{1/2,\Gamma_C} \leq C \|v\|_{1,\Omega^1,\Omega^2}.$$

■

We observe that the research of sufficient conditions on the meshes in order to construct the stable average preserving operator π_1^h is similar to the research of discrete approximation spaces satisfying the inf-sup condition. Besides note that the three-dimensional refinement procedure proposed for tetrahedra and hexahedra (whose aim is to obtain a simple macro-mesh) could also be chosen in the linear two-dimensional case by dividing any contact element in two elements but this is not necessary since it is simpler (and equivalent) to consider a segment with two contact elements as in Section 2.

Remark 11 *Here we can see some similarities (in the linear case) with the discontinuous mortar domain decomposition studied in [30, 31] when considering its adaptation to the contact problem. The main difference is that the inf-sup condition directly comes from the definition of the macro-mesh T^M instead of being fulfilled by the introduction of a bubble enrichment of one of the approximation space V_ℓ^h.*

4.3 Error estimate

The following theorem shows that we can obtain the same convergence rates for the solution to the mixed problem (31) than those stated in Theorem 1 and Theorem 2 for the variational inequality problem.

Theorem 3 *Let $(u, \lambda = \sigma_{_N})$ and (u^h, λ^h) be the solutions to the continuous Problem (7) and to the discrete Problem (31) respectively. Let $d = 2, 3$ and $k = 1, 2$. Assume that Hypothesis 1 is verified when $d = 3$ and that $u \in (H^\tau(\Omega^1))^d \times (H^\tau(\Omega^2))^d$ with $3/2 < \tau \leq \min(k+1, 5/2)$. Then, there exists a constant $C > 0$ independent of $h = (h_1, h_2)$ and u such that*

$$\|\lambda - \lambda^h\|_{1/2,*,\Gamma_C} + \|u - u^h\|_{1,\Omega^1,\Omega^2} \leq C(h_1^{\tau-1} + h_2^{\tau-1})\|u\|_{\tau,\Omega^1,\Omega^2},$$

where $\|.\|_{1/2,*,\Gamma_C}$ stands for the dual norm of $\|.\|_{1/2,\Gamma_C}$.

Proof. The proof is straightforward and standard. Since the inf-sup condition (39) is verified it only remains to bound similar terms to the ones bound in the proof of Theorems 1 and 2 (see, e.g., [34]).

■

5 Numerical experiments

The LAC method has been implemented in the finite element software of Electricité de France (EDF), ***Code_Aster***. For more than 20 years, this FE code is both the repository of the research in solid and structure mechanics led at the R&D department of EDF and the simulation tool used by the engineering divisions to analyze various components of the power plants (nuclear, hydraulic...) and also to justify safety for the French nuclear safety authority (ASN).

We use an already implemented full non linear algorithm, see [41]. All the non linearities (material behavior, geometrical, and contact) are solved inside a single Newton loop. At each Newton step we perform a geometrical update and a contact pairing detection (segment-to-segment pairing quite similar to the one in [48] with a search method based on [26]), and then we construct and solve the linear system, see Figure 4. The locality of the proposed method allows us to easily compute the linear system (at each Newton step) at an elementary level. The only prerequisite to be satisfied is the fulfillment of the Hypothesis 1. This is accomplished thanks

to a local pretreatment on the contact zone, see Figures 2, 3. So we are able to implement the LAC method in an easy an generic way for the most common finite elements in 2D (3-node linear and 6-node quadratic triangles, 4-node bi-linear and 8-node bi-quadratic quadrangles) and in 3D (4-node linear and 10-node quadratic tetrahedra, 8-node bi-linear, 20 and 27-node bi-quadratic hexahedra). More details on the numerical implementation are available in [20].

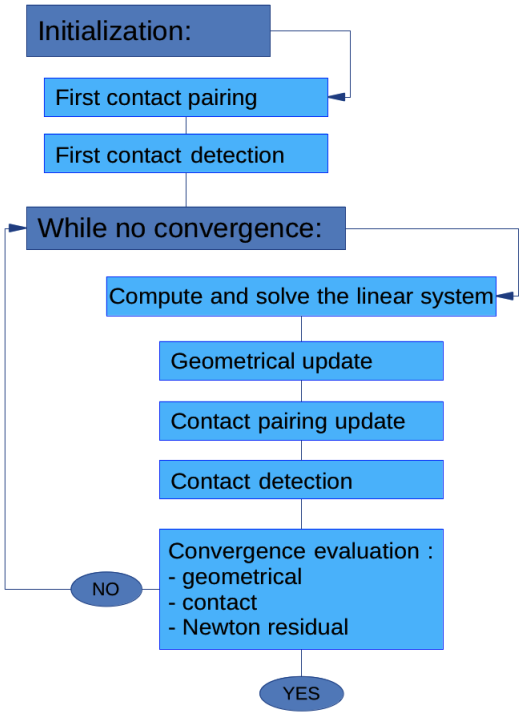

Figure 4: One Newton loop algorithm.

In this section, we analyze the behavior (in 2D and 3D) of the method facing the well-known contact problems: the Taylor patch test and the Hertzian contact. To conclude the numerical experiments, we will take a look at the numerical convergence rates.

5.1 Taylor patch test

5.1.1 Test configuration in 2D

We consider a structure which consists of two identical squares of edge lengths $50mm$ having a common horizontal edge which is the contact area Γ_C. The material characteristics are: a Young modulus $E = 2000MPa$ and a Poisson ratio $\nu = 0.3$. We set symmetric conditions both on the left part and on the lower part of the structure and apply a $25MPa$ pressure at the top of the upper square. Both squares are meshed independently with 3-node triangles or 4-node quadrangles which leads to nonmatching trace meshes on the contact zone (see Figures 5 to 7). In this case the solution u to the continuous problem is linear and the stress field σ_{yy} in the structure as well as the contact pressure $\sigma_{_N}$ are constant and equal to $25MPa$. The mortar

method is known to pass successfully this Taylor patch test whereas other methods based on node-to-segment approaches fail when considering the general case of nonmatching meshes (see, e.g., [33, 52]). Before computing the results with the LAC method, we consider in Figure 5 the solutions obtained with a node-to-segment method. We see that the Lagrange multiplier (contact pressure) and the stress field σ_{yy} around the contact zone show some oscillations (range between $24.2MPa$ and $25.6MPa$). So the node-to-segment method does not satisfy the Taylor patch test in a satisfactory way.

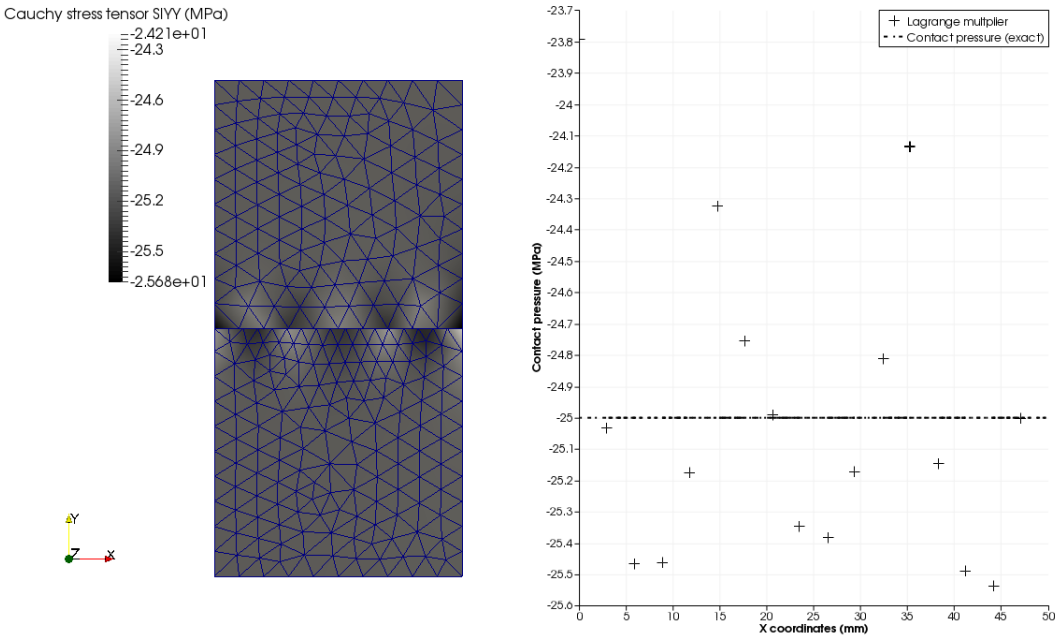

Figure 5: Numerical results obtained with a standard node-to-segment method in 2D when considering 3-node triangles: on the left σ_{yy} on the deformed shape (scale factor 10), on the right Lagrange multipliers on Γ_C.

The numerical results obtained with the LAC condition are depicted in Figures 6 and 7. We get the expected results on the displacement field, the Lagrange multiplier equals $25 \pm 10^{-9} MPa$ on Γ_C, the gap numerically vanishes on Γ_C and the Cauchy stress tensor component σ_{yy} equals $25 \pm 10^{-9} MPa$ in the structure.

Remark 12 *We see in Figure 6 that the elements of the trace mesh on Γ_C of the lower square (which stands for Ω^1) are gathered by pairs to form the macro-mesh I^M. There are 34 elements in the trace mesh of the lower square and the Lagrange multiplier space $P_0(I^M)$ admits 17 d.o.f.*

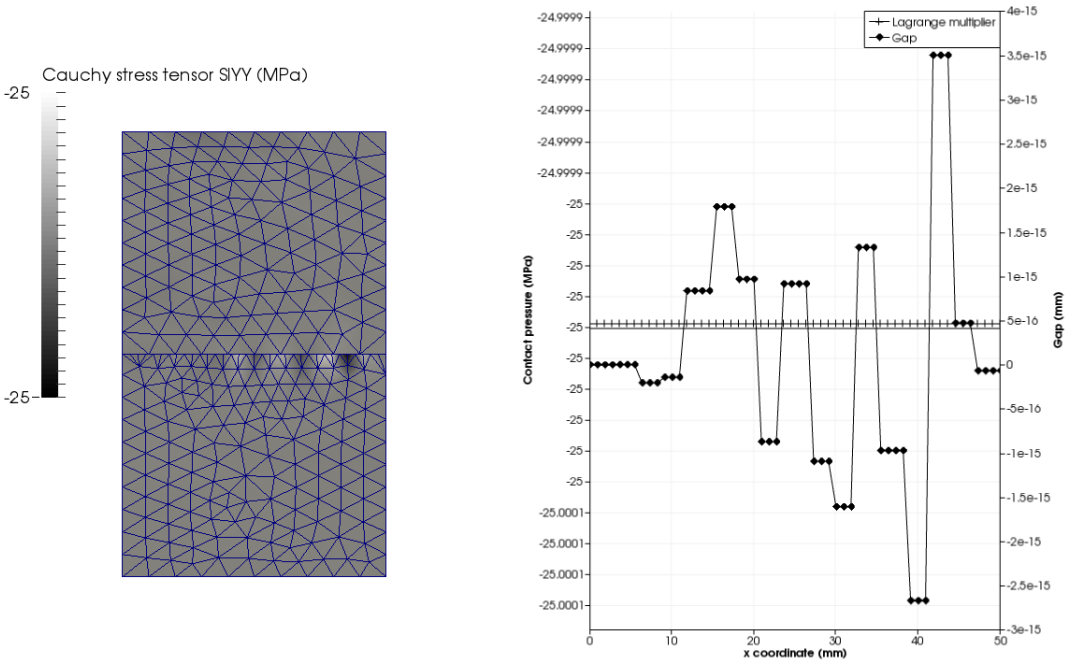

Figure 6: Numerical results obtained with the LAC condition in 2D when considering 3-node triangles: on the left σ_{yy} on the deformed shape (scale factor 10), on the right Lagrange multipliers and gap on Γ_C.

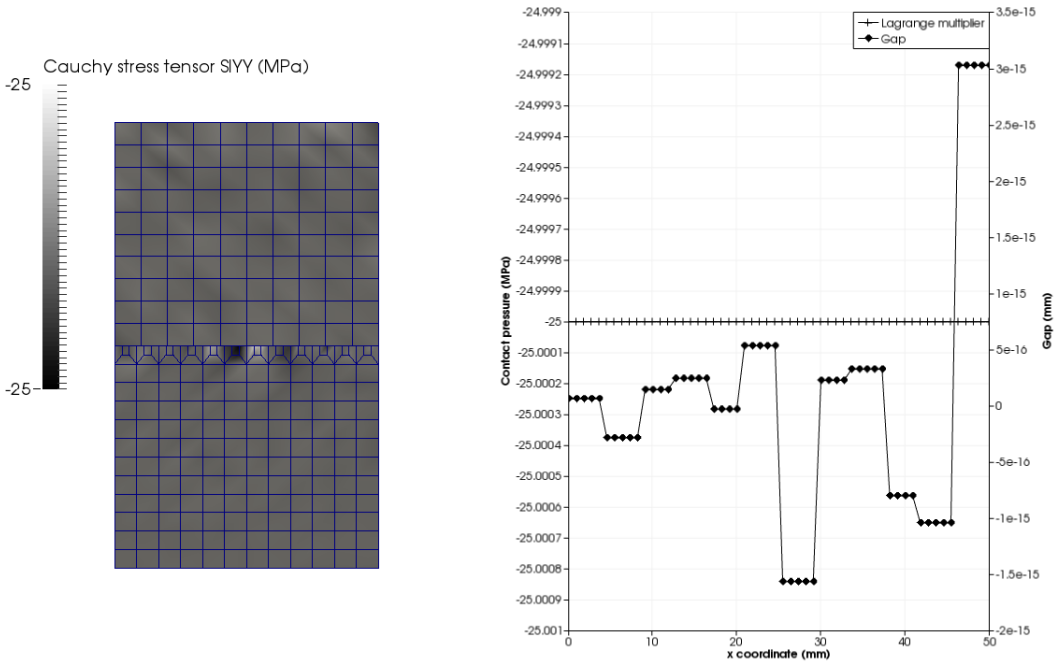

Figure 7: Numerical results obtained with the LAC condition in 2D when considering 4-node quadrangles: on the left σ_{yy} on the deformed shape (scale factor 10), on the right Lagrange multipliers and gap on Γ_C.

5.1.2 Test configuration in 3D

We now consider a structure which consists of two identical cubes of edge lengths $50mm$ having a common horizontal face which is the contact area Γ_C. The material characteristics are the same as previously: a Young modulus $E = 2000MPa$ and a Poisson ratio $\nu = 0.3$ are chosen. We set symmetric conditions on the two vertical faces $\overrightarrow{Ox}\overrightarrow{Oz}$ and $\overrightarrow{Oy}\overrightarrow{Oz}$ and on the lower part of the structure (Oz stands for the vertical axis). We apply a $25MPa$ pressure at the top of the upper cube. Both cubes are meshed independently with 4-node tetrahedra or 8-node hexahedra with nonmatching trace meshes on the contact zone (see Figures 8 and 9).
As in the two-dimensional case, the solution u to the continuous problem is known (linear displacement fields, constant σ_{zz} field and constant Lagrange multipliers both equal to $25MPa$). The results are depicted in Figures 8 and 9. We obtain the expected results on the displacement field, the contact pressure (Lagrange multipliers) equals $25 \pm 10^{-9}MPa$ on Γ_C and Cauchy stress tensor component σ_{zz} equals $25 \pm 10^{-9}MPa$ in the structure.

Remark 13 *In the right picture of Figures 8 and 9, we can see the result of the pre-processing work which ensures that the trace mesh on the slave side of the contact zone (i.e., the mesh of* Ω^1 *on* Γ_C*) satisfies Hypothesis 1.*

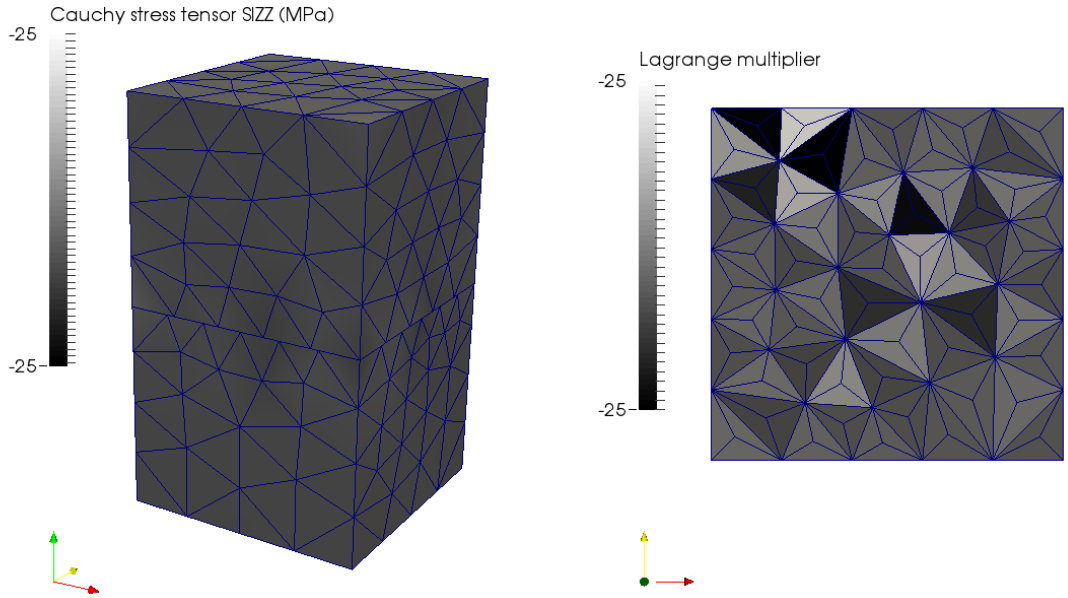

Figure 8: Numerical results obtained with the LAC condition in 3D when considering 4-node tetrahedra: on the left σ_{zz} on the deformed shape (scale factor 10), on the right Lagrange multipliers on Γ_C.

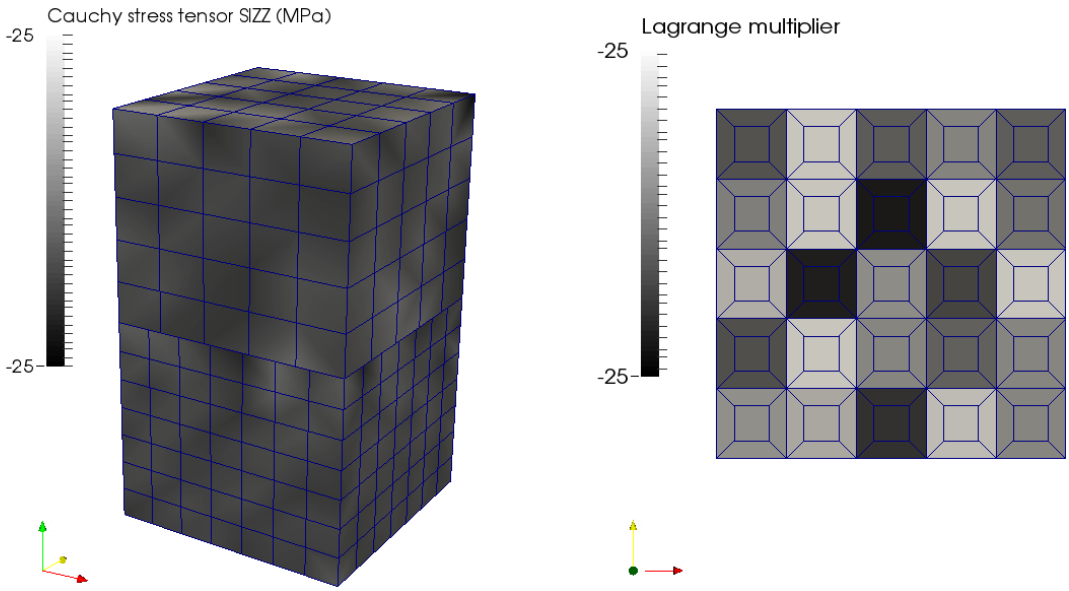

Figure 9: Numerical results obtained with the LAC condition in 3D when considering 8-node hexahedra: on the left σ_{zz} on the deformed shape (scale factor 10), on the right Lagrange multipliers on Γ_C.

5.2 Hertzian contact

5.2.1 Test configuration in 2D

The aim of this example is to adapt the local average contact procedure to a more general context than the theoretical convergence framework (vanishing initial gap and Γ_C is a straight line segment). We consider a benchmark for contact problems taken from [38]: a structure which consists of a cylinder (diameter equal to $100mm$, $E = 2.1 \cdot 10^5 MPa$ and $\nu = 0.3$) contacting a square foundation (edge length equal to $200mm$, $E = 7 \cdot 10^7 MPa$ and $\nu = 0.3$). We use a symmetric condition on the $\overrightarrow{Oy}$ axis and we apply a vertical point load on the top of the cylinder ($F = 35kN$). In such a configuration, we have to consider nonmatching meshes, on account of the geometries of the bodies. Moreover, there is an initial gap and consequently, there are points of the boundaries initially not in contact which will come into contact after deformation. Note that the continuous noninterpenetration condition in (5) becomes $[u_N] - g \leq 0$ where g is the intial gap between both bodies. So the discrete contact condition in (8) becomes $\int_{I^m} ([v_N^h] - g^h)\, d\Gamma \leq 0$ where g^h is a suitable finite element approximation of the gap function.

This benchmark allows us to test our method when considering a geometric non-linearity and non-linear boundary conditions (deformable-deformable contact with status transition in the supposed contact area) together with quadratic elements. An analytical solution is known for the contact pressure and presented in [38]: we recall that the contact pressure should be equal to

$$p(x) = p_{max} \sqrt{1 - \frac{x^2}{a}}$$

where $p_{max} = -3585.37MPa$, and the half contact width a equals $6.21mm$. Both objects are meshed independently with 6-node triangles or 8-node quadrangles with nonmatching trace meshes on the contact zone (see Figures 10 to 12). Before computing with the LAC method, we first show in Figure 10 the solutions obtained with a node-to-segment method. As expected the Lagrange multiplier and the Von Mises stresses around the contact zone show some oscillations.

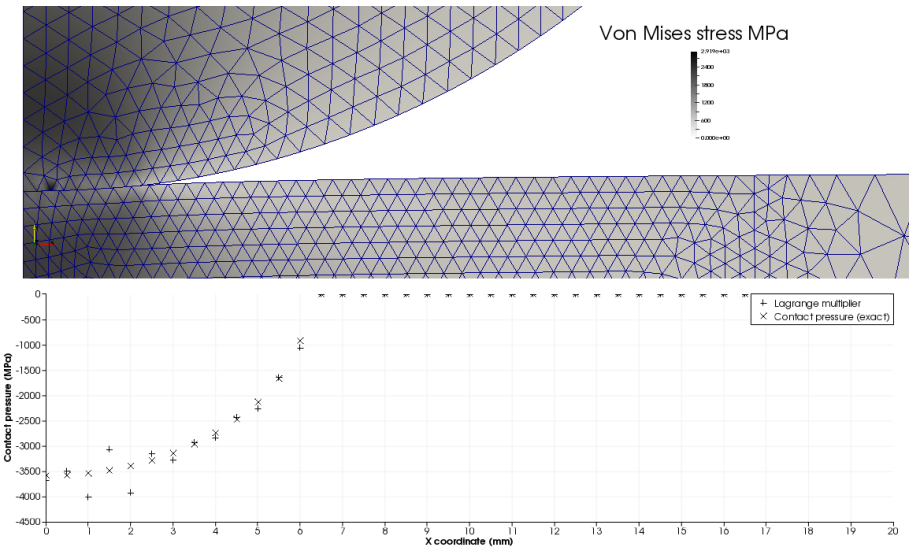

Figure 10: Numerical results obtained with a standard node-to-segment method in 2D when considering 6-node triangles: Von Mises stress on the deformed shape (top). Exact contact pressure (interpolated on the trace mesh) and computed Lagrange multiplier (bottom).

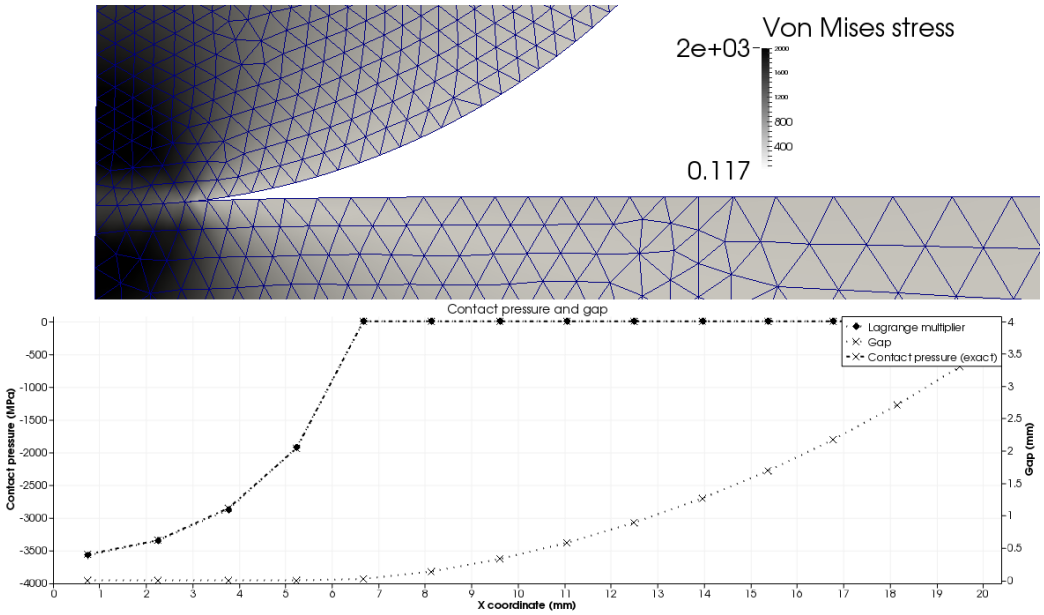

Figure 11: Numerical results obtained with the LAC condition in 2D when considering 6-node triangles: Von Mises stress on the deformed shape (top). Exact Lagrange multiplier (interpolated on the trace mesh), computed Lagrange multiplier and gap (bottom).

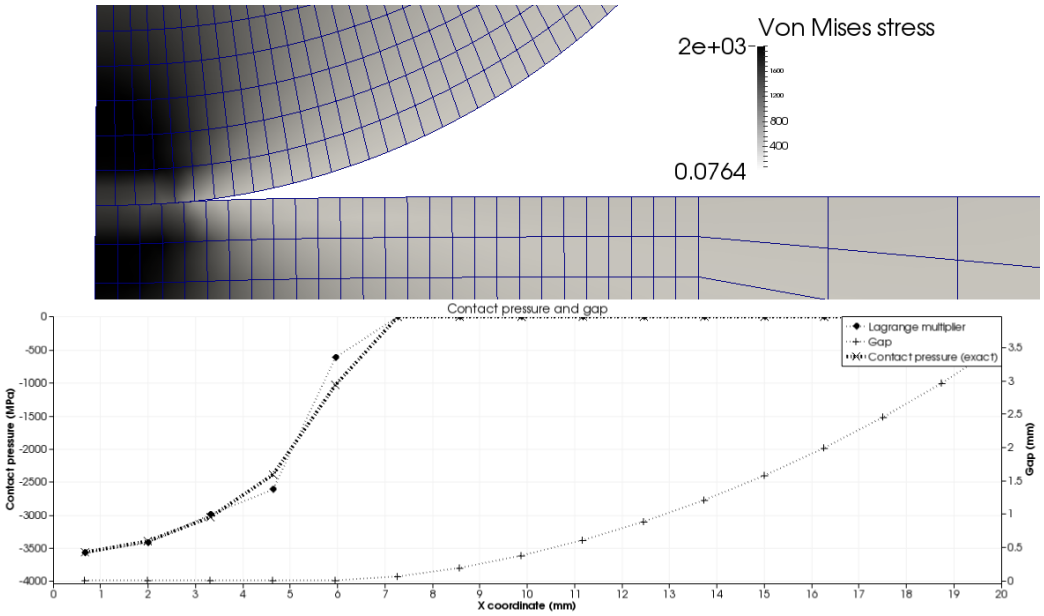

Figure 12: Numerical results obtained with the LAC condition in 2D when considering 8-node quadrangles: Von Mises stress on the deformed shape (top). Exact Lagrange multiplier (interpolated on the trace mesh), computed Lagrange multiplier and gap (bottom).

The results using the LAC method are depicted in Figures 11 and 12. We get the expected results on the Lagrange multipliers. There is a slight error of 0.21% on p_{max} in the 6-node triangles case and of 0.35% in the 8-node quadrangles case. Since the contact status is only known in average on every macro-element the approximation of the contact area half width is not as accurate as the one given by approach based on nodal contact status ("node-to-segment" or "standard mortar" approaches). Nevertheless, we still get an estimate in good agreement with the analytical solution, the computed half width a ranges between $5.94mm$ and $7.26mm$ when considering 6-node triangles and $5.22mm$ and $6.66mm$ when considering 8-node quadrangles. Note that there are only 4 or 5 true contacting elements, we could get even better results by considering a finer mesh on the contact zone, especially if we want accurate results for the approximation of the contact area half width.

5.2.2 Test configuration in 3D

We now consider two half spheres (radius equal to $100mm$, $E = 2000MPa$, and $\nu = 0.3$), we set symmetric conditions on the two vertical faces $\overrightarrow{Ox}\overrightarrow{Oz}$ and $\overrightarrow{Oy}\overrightarrow{Oz}$ (so we only modeled one eighth of each sphere), we apply a vertical displacement of $-1.5mm$ on the top of the upper sphere and respectively $1.5mm$ at the bottom of the lower sphere. An analytical solution is known for the contact pressure (see [22]): we recall that the contact pressure should be equal to

$$p(r) = p_{max}\sqrt{1 - \frac{r}{a}^2}$$

where $p_{max} = -171.362MPa$, and the half contact width a equals $12.247mm$. It is also known that the maximum Von Mises stress should be observed near the contact zone inside the half

spheres. As previously, both objects are meshed independently with 10-node tetrahedra, or 20-node hexahedra, or 27-node hexahedra with nonmatching trace meshes on the contact zone (see Figures 13, 14 and 15). The results are depicted in Figures 13, 14 and 15.
We observe a good agreement between the numerical results and the analytical ones. The error on p_{max} ranges between 1.9% and 2.3% depending on the kind and the number of elements used (see also Remark 14). We also get a good localization of the maximum of Von Mises stress. As in the previous case, the detection of the contact half width a is not as accurate as the one obtained with a nodal based contact condition. We obtain a computed a for the finer mesh (10-node tetrahedra) which ranges between $12.29mm$ and $12.55mm$. Although the contact contribution is only taken into account on a macro-element scale, we get a good circular shape for the contact area and the expected parabolic contact pressure distribution across this area without any noticeable oscillations as the ones that could occur when using a "node-to-face" approach.

Remark 14 *A part of the error on the maximum contact pressure p_{max} is due to the full non-linear algorithm used to solve the problem. This algorithm takes into account all the "small" non linearities coming from the contact geometry. So, these non-linear contributions slightly take us away from the small strain conditions which are used to get the exact solution. We notice that this "gap" with the analytical contact pressure is more noticeable in the 3D case than in the 2D case.*

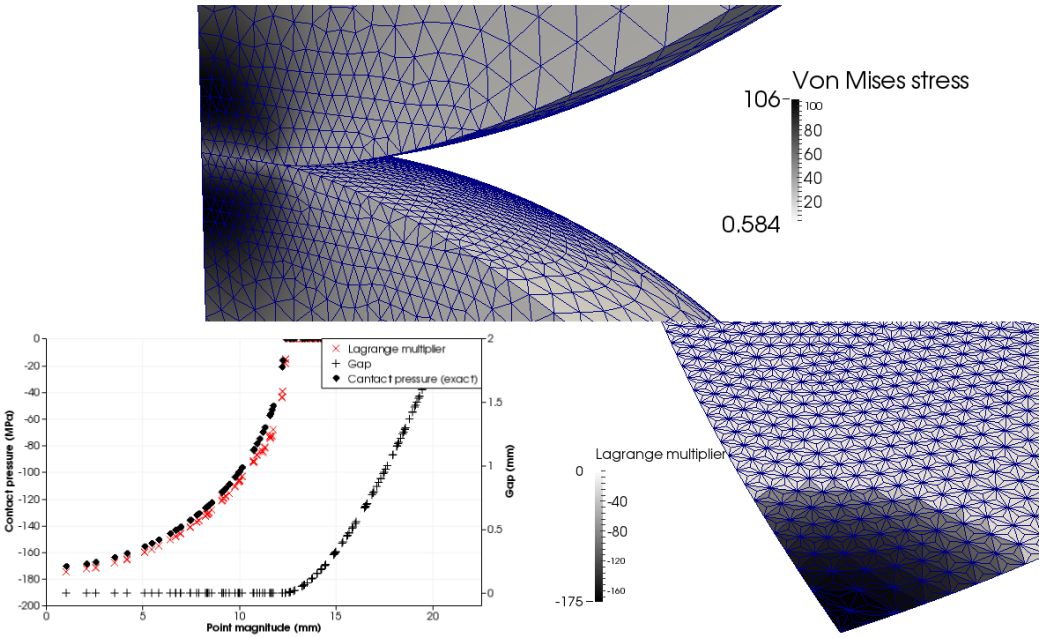

Figure 13: Numerical results obtained with the LAC condition in 3D when considering 10-node tetrahedra: Von Mises stress on the deformed shape (top). Exact Lagrange multiplier (interpolated on the trace mesh), computed Lagrange multiplier and gap (bottom left). Trace mesh on Γ_C and computed Lagrange multiplier (bottom right).

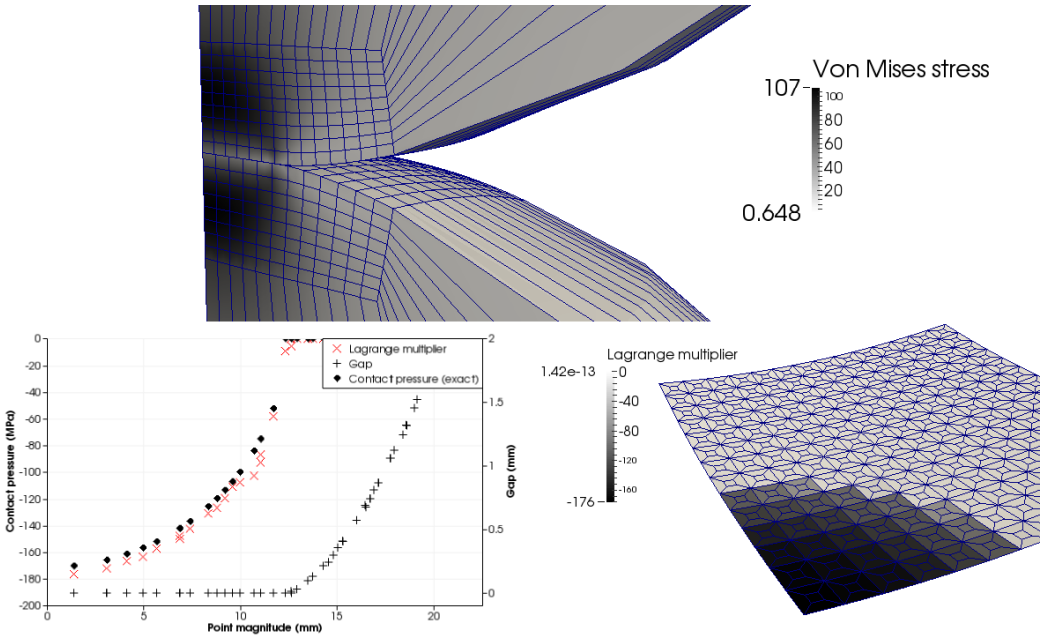

Figure 14: Numerical results obtained with the LAC condition in 3D when considering 20-node hexahedra: Von Mises stress on the deformed shape (top). Exact Lagrange multiplier (interpolated on the trace mesh), computed Lagrange multiplier and gap (bottom left). Trace mesh on Γ_C and computed Lagrange multiplier (bottom right).

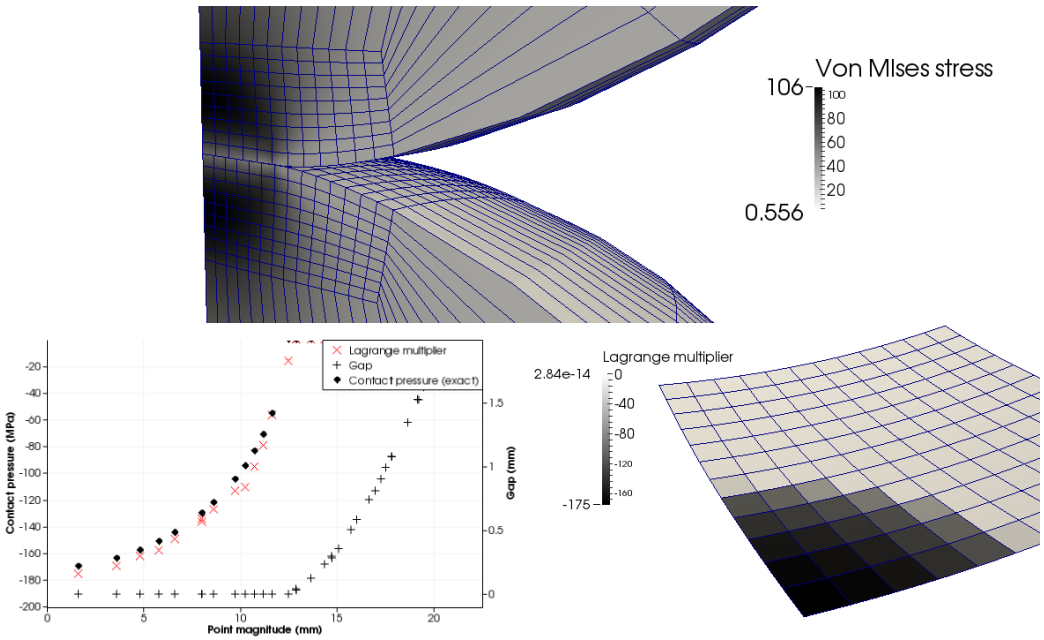

Figure 15: Numerical results obtained with the LAC condition in 3D when considering 27-node hexahedra: Von Mises stress on the deformed shape (top). Exact Lagrange multiplier (interpolated on the trace mesh), computed Lagrange multiplier and gap (bottom left). Trace mesh on Γ_C and computed Lagrange multiplier (bottom right).

5.2.3 Numerical convergence rates

Setting of the test We study the numerical convergence rates of the LAC method and we compare them with the theoretical ones. We consider the Hertzian contact configuration introduced previously in both the 2D and the 3D cases. We compute the L^2-error in displacement $\|u-u^h\|_{0,\Omega^1,\Omega^2}$ and the L^2-error on the contact pressure $\|\lambda-\lambda^h\|_{0,\Gamma_C}$ (seen as a Lagrange multiplier). Although there is to our knowledge no proof of optimal $L^2(\Omega^1\cup\Omega^2)$-error decay on the displacements (the only partial existing results can be found in [16, 51]) we can nevertheless expect (or believe) that this error behaves like $(h_1+h_2)\|u-u^h\|_{1,\Omega^1,\Omega^2}$ as in the linear case where the Aubin-Nitsche argument can be applied. So we compare our numerical convergence rates with these unproved and expected optimal theoretical rates.

Concerning the $L^2(\Gamma_C)$-error on the Lagrange multiplier the situation is simpler. By using standard results (inverse inequality and approximation properties as in [16, 51]) we easily obtain from Theorem 3:

$$\|\lambda-\lambda^h\|_{0,\Gamma_C}\leq Ch_1^{-1/2}(h_1^{\tau-1}+h_2^{\tau-1})\|u\|_{\tau,\Omega^1,\Omega^2},$$

where $3/2<\tau\leq\min(k+1,5/2)$.

Since there does not exist an analytical solution for the displacement field u we will use a numerical reference solution computed with a sufficiently fine mesh. All the results are reported in Tables 1 and 2 for the 2D and the 3D cases respectively. Even though the test cases are tough (geometrical non linearity, contact transition, small effective contact zone, deformable-deformable contact), the numerical convergence rates can be compared with the expected ones.

Element type	$\|u-u^h\|_{0,\Omega^1,\Omega^2}$		$\|\lambda-\lambda^h\|_{0,\Gamma_C}$	
	Expected	Numerical	Expected	Numerical
3-node triangle	*2.0*	2.33	*0.5 (1)*[3]	0.71
6-node triangle	*2.5*	3.11	*1.0*	0.91
4-node quadrangle	*2.0*	2.04	*0.5 (1)*	0.76
8-node quadrangle	*2.5*	2.24	*1.0*	0.83

Table 1: Convergence rates in the 2D case

Element type	$\|u-u^h\|_{0,\Omega^1,\Omega^2}$		$\|\lambda-\lambda^h\|_{0,\Gamma_C}$	
	Expected	Numerical	Expected	Numerical
4-node tetrahedron	*2.0*	1.97	*0.5 (1)*	0.83
10-node tetrahedron	*2.5*	2.42	*1.0*	0.97
8-node hexahedron	*2.0*	2.24	*0.5 (1)*	0.83
20-node hexahedron	*2.5*	2.36	*1.0*	0.95
27-node hexahedron	*2.5*	2.30	*1.0*	0.99

Table 2: Convergence rates in the 3D case

[3] In a recent paper [51] the authors prove for a standard conforming linear finite element approximation of the Signorini problem in 2D and 3D that the $L^2(\Gamma_C)$-error bound on the multipliers could be improved with a factor $h^{1/2}$. This could explain the better convergence we observe in our framework which is very close to that considered in [51].

6 Conclusion

In order to handle nonmatching meshes on the contact interface between two and three-dimensional elastic bodies, we propose a method using a simple local average noninterpenetration condition for various linear and quadratic finite elements. In the case of the two-dimensional unilateral contact problem the Local Average Contact (LAC) condition allows us to obtain optimal convergence results without any other assumption than the Sobolev regularity of the continuous solution u (as the standard approaches considered with matching meshes, see [21]). Note that the standard mortar approach would also give optimal bounds by using the results of [21]. In the three-dimensional case, our method only requires a minor hypothesis on the mesh (i.e., the averages must be computed on patches containing at least the support of a basis function) to extend the two-dimensional optimal results. These results for non matching meshes are mostly due to the operator π_h^1 developed to tackle the error analysis when considering the local average contact condition. The first numerical results, considering 3 and 6-node triangles, 4 and 8-node quadrangles in the 2D case and 4 and 10-node tetrahedra, 8, 20 and 27-node hexahedra in the 3D case, confirm the good behavior of the LAC method and its "developer-friendly" implementation in an industrial FE code. Further numerical experiments and the extension to the dynamic and friction cases should be considered.

References

[1] J. Andersson. Optimal regularity for the Signorini problem and its free boundary. *St. Petersburg Mathematical Journal*, 24:371–386, 2013.

[2] I. Athanasopoulos and L. A. Caffarelli. Optimal regularity of lower dimensional obstacle problems. *J. Math. Sci. (N. Y.)*, 132(3):274–284, 2006.

[3] S. Auliac, Z. Belhachmi, F. Ben Belgacem, and F. Hecht. Quadratic finite elements with non-matching grids for the unilateral boundary contact. *ESAIM: Mathematical Modelling and Numerical Analysis*, 47(4):1185–1205, 2013.

[4] G. Bayada, M. Chambat, K. Lhalouani, and T. Sassi. Éléments finis avec joints pour des problèmes de contact avec frottement de Coulomb non local. (french) [on the mortar finite element method for contact problems with nonlocal Coulomb law]. *C. R. Acad. Sci. Paris Sér. I Math.*, 325(12):1323–1328, 1997.

[5] F. Ben Belgacem and S. C. Brenner. Some nonstandard finite element estimates with applications to 3D Poisson and Signorini problems. *Electronic Transactions on Numerical Analysis*, 12:134–148, 2001.

[6] F. Ben Belgacem, P. Hild, and P. Laborde. Approximation of the unilateral contact problem by the mortar finite element method. *Comptes Rendus de l'Academie des Sciences Series I Mathematics*, 324(1):123–127, 1997.

[7] F. Ben Belgacem, P. Hild, and P. Laborde. Extension of the mortar finite element method to a variational inequality modeling unilateral contact. *Mathematical Models and Methods in Applied Sciences*, 9(2):287–303, 1999.

[8] F. Ben Belgacem and Y. Renard. Hybrid finite element methods for the Signorini problem. *Mathematics of Computation*, 72(243):1117–1145, 2003.

[9] C. Bernardi and V. Girault. A local regularization operator for triangular and quadrilateral finite elements. *SIAM Journal on Numerical Analysis*, 35:1893–1916, 1998.

[10] C. Bernardi, Y. Maday, and A. T. Patera. A new non conforming approach to domain decomposition: The mortar element method. In H. Brezis and J.-L. Lions, editors, *Collège de France Seminar*, pages 13–51. Pitman, 1994.

[11] S. C. Brenner and R. Scott. *The mathematical theory of finite element methods*, volume 15. Springer, 2008.

[12] Z. Chen and R. H. Nochetto. Residual type a posteriori error estimates for elliptic obstacle problems. *Numerische Mathematik*, 84(4):527–548, 2000.

[13] A. Chernov, M. Maischak, and E. P. Stephan. hp-mortar boundary element method for two-body contact problems with friction. *Mathematical Methods in the Applied Sciences*, 31(17):2029–2054, 2008.

[14] P. G. Ciarlet. *The finite element method for elliptic problems*. Elsevier, 1978.

[15] T. Cichosz and M. Bischoff. Consistent treatment of boundaries with mortar contact formulations using dual Lagrange multipliers. *Computer Methods in Applied Mechanics and Engineering*, 200(9):1317–1332, 2011.

[16] P. Coorevits, P. Hild, K. Lhalouani, and T. Sassi. Mixed finite element methods for unilateral problems: convergence analysis and numerical studies. *Mathematics of Computation*, 71(237):1–25, 2002.

[17] M. Crouzeix and V. Thomée. The stability in l^p and of $w^{1,p}$ the l^2-projection onto finite element function spaces. *Mathematics of Computation*, 48(178):521–532, 1987.

[18] Electricité de France. Finite element *Code_Aster*, analyses de structures Thermo-Elastiques pour des Etudes et des Recherches. Open source on www.code-aster.org, 1989–2015.

[19] Z. Dostál, D. Horák, and D. Stefanica. A scalable feti–dp algorithm with non-penetration mortar conditions on contact interface. *Journal of Computational and Applied Mathematics*, 231(2):577–591, 2009.

[20] G. Drouet. *Méthode locale de type mortar pour le contact dans le cas de maillages incompatibles de degré élevé*. PhD thesis, Université Paul Sabatier, (http://thesesups.ups-tlse.fr/2897/1/2015TOU30142.pdf), 2015.

[21] G. Drouet and P. Hild. Optimal convergence for discrete variational inequalities modelling Signorini contact in 2D and 3D without additional assumptions on the unknown contact set. *SIAM Journal on Numerical Analysis*, 53(3):1488–1507, 2015.

[22] G. Dumont. Algorithme des contraintes actives et contact unilatéral sans frottement. *Revue Européenne des Eléments Finis, Hermès*, 4(1):55–73, 1995.

[23] A. Ern and J. L. Guermond. *Theory and practice of finite elements*. Springer-Verlag, New York, Inc., 2004.

[24] P. Farah, A Popp, and W. A. Wall. Segment-based vs. element-based integration for mortar methods in computational contact mechanics. *Comput. Mech.*, 55(1):209–228, 2015.

[25] G. Fichera. Problemi elastostatici con vincoli unilaterali: il problema di Signorini con ambigue condizioni al contorno. *Atti Accad. Naz. Lincei Mem. Cl. Sci. Fis. Mat. Natur. Sez. I*, 7(8):91–140, 1963/1964.

[26] M. J. Gander and C. Japhet. Algorithm 932: Pang: software for nonmatching grid projections in 2d and 3d with linear complexity. *ACM Transactions on Mathematical Software (TOMS)*, 40(1):6, 2013.

[27] N. Guillen. Optimal regularity for the Signorini problem. *Calc. Var. Partial Differential Equations*, 36:533–546, 2009.

[28] S. Hartmann and E. Ramm. A mortar based contact formulation for non-linear dynamics using dual Lagrange multipliers. *Finite Elements in Analysis and Design*, 44(5):245–258, 2008.

[29] J. Haslinger, I. Hlavácek, and J. Necas. *Numerical methods for unilateral problems in solid mechanics*, volume 4 of *Handbook of Numerical Analysis*. North-Holland, Amsterdam, 1996.

[30] P. Hauret and P. Le Tallec. A stabilized discontinuous mortar formulation for elastostatics and elastodynamics problems, Part 2: discontinuous Lagrange multipliers. Technical report, CMAP, 2004.

[31] P. Hauret and P. Le Tallec. A discontinuous stabilized mortar method for general 3D elastic problems. *Computer Methods in Applied Mechanics and Engineering*, 196(49):4881–4900, 2007.

[32] P. Hild. *Problèmes de contact unilatéral et maillages éléments finis incompatibles*. PhD thesis, Université Paul Sabatier, (www.math.univ-toulouse.fr/∼phild/), 1998.

[33] P. Hild. Numerical implementation of two nonconforming finite element methods for unilateral contact. *Computer Methods in Applied Mechanics and Engineering*, 184(1):99–123, 2000.

[34] P. Hild and P. Laborde. Quadratic finite element methods for unilateral contact problems. *Applied Numerical Mathematics*, 41(3):401–421, 2002.

[35] P. Hild and Y. Renard. A stabilized Lagrange multiplier method for the finite element approximation of contact problems in elastostatics. *Numerische Mathematik*, 115(1):101–129, 2010.

[36] S. Hüeber and B. I. Wohlmuth. A primal-dual active set strategy for non-linear multibody contact problems. *Comput. Methods Appl. Mech. Engrg.*, 194(27–29):3147–3166, 2005.

[37] N. Kikuchi and J. T. Oden. *Contact problems in elasticity: a study of variational inequalities and finite element methods*. SIAM, 1988.

[38] A. Konter. Advanced finite element contact benchmarks. *NAFEMS*, 2006.

[39] R. Krause. A nonsmooth multiscale method for solving frictional two-body contact problems in 2D and 3D with multigrid efficiency. *SIAM Journal on Scientific Computing*, 31(2):1399–1423, 2009.

[40] R. H. Krause and B. I. Wohlmuth. Monotone multigrid methods on nonmatching grids for nonlinear multibody contact problems. *SIAM J. Sci. Comput.*, 25(1):324–347, 2003.

[41] A. D. Kudawoo. *Problèmes industriels de grande dimension en mécanique numérique du contact : performance, fiabilité et robustesse.* PhD thesis, Aix-Marseille, (https://tel.archives-ouvertes.fr/tel-00773642/document), 2012.

[42] T. A. Laursen. *Computational contact and impact mechanics: fundamentals of modeling interfacial phenomena in nonlinear finite element analysis.* Springer, 2002.

[43] T. A. Laursen, M. A. Puso, and J. Sanders. Mortar contact formulations for deformable–deformable contact: past contributions and new extensions for enriched and embedded interface formulations. *Computer Methods in Applied Mechanics and Engineering*, 205:3–15, 2012.

[44] J.-L. Lions and E. Magenes. *Problemes aux limites non homogenes et applications*, volume 1. Dunod, 1968.

[45] M. Moussaoui and K. Khodja. Régularité des solutions d'un problème mêlé Dirichlet–Signorini dans un domaine polygonal plan. *Communications in Partial Differential Equations*, 17(5-6):805–826, 1992.

[46] A. Popp, B. I. Wohlmuth, M. W. Gee, and W. A. Wall. Dual quadratic mortar finite element methods for 3D finite deformation contact. *SIAM Journal on Scientific Computing*, 34(4):B421–B446, 2012.

[47] M. A. Puso and T. A. Laursen. A mortar segment-to-segment frictional contact method for large deformations. *Computer Methods in Applied Mechanics and Engineering*, 193(45-47):4891–4913, 2004.

[48] M. A. Puso, T. A. Laursen, and J. Solberg. A segment-to-segment mortar contact method for quadratic elements and large deformations. *Computer Methods in Applied Mechanics and Engineering*, 197(6):555–566, 2008.

[49] L.R. Scott and S. Zhang. Finite element interpolation of nonsmooth functions satisfying boundary conditions. *Math. Comp.*, 54:483–493, 1990.

[50] A. Signorini. Questioni di elastostatica linearizzata e semilinearizzata. *Rend. Math*, 18:381–402, 1959.

[51] O. Steinbach, B. I. Wohlmuth, and L. Wunderlich. Trace and flux a priori error estimates in the finite element approximations of Signorini-type problems. *IMA Journal of Numerical Analysis*, 2015. doi:10.1093/imanum/drv039.

[52] R. L. Taylor and P. Papadopoulos. On a patch test for contact problems in two dimensions. *Computational Methods in Nonlinear Mechanics*, pages 690–702, 1991.

[53] I. Temizer. A mixed formulation of mortarbased contact with friction. *Computer Methods in Applied Mechanics and Engineering*, 255:183–195, 2013.

[54] I. Temizer, P. Wriggers, and T.J.R. Hughes. Three-dimensional mortarbased frictional contact treatment in isogeometric analysis with NURBS. *Computer Methods in Applied Mechanics and Engineering*, 209/212:115–128, 2012.

[55] H. Triebel. *Interpolation theory, function spaces, differential operators*. North-Holland, 1978.

[56] M. Tur, F. J. Fuenmayor, and P. Wriggers. A mortar-based frictional contact formulation for large deformations using Lagrange multipliers. *Computer Methods in Applied Mechanics and Engineering*, 198(37):2860–2873, 2009.

[57] B. I. Wohlmuth. Variationally consistent discretization schemes and numerical algorithms for contact problems. *Acta Numerica*, 20:569–734, 2011.

[58] B. I. Wohlmuth, A. Popp, M. W. Gee, and W. A. Wall. An abstract framework for a priori estimates for contact problems in 3D with quadratic finite elements. *Computational Mechanics*, 49(6):735–747, 2012.

[59] P. Wriggers. *Computational contact mechanics*. Springer, 2006.